

Signaling Design of Two-Way MIMO Full-Duplex Channel: Optimality Under Imperfect Transmit Front-End Chain

Shuqiao Jia and Behnaam Aazhang,

Abstract

We derive the optimal signaling for a multiple input multiple output (MIMO) full-duplex two-way channel under the imperfect transmit front-end chain. We characterize the two-way rates of the channel by using a game-theoretical approach, where we focus on the Pareto boundary of the achievable rate region and Nash equilibria (NE). For a MISO full-duplex two-way channel, we prove that beamforming is an optimal transmission strategy which can achieve any point on the Pareto boundary. Furthermore, we present a closed-form expression for the optimal beamforming weights. In our numerical examples we quantify gains in the achievable rates of the proposed beamforming over the zero-forcing beamforming. For a general MIMO full-duplex channel, we establish the existence of NE and present a condition for the uniqueness of NE. We then propose an iterative water-filling algorithm which is capable of reaching NE. Through simulations the threshold of the self-interference level is found, below which the full-duplex NE outperforms the half-duplex TDMA.

Index Terms

full duplex two-way channel, MIMO, transmit front-end noise, Beamforming, Pareto boundary, Nash equilibrium.

I. INTRODUCTION

A node in a full-duplex mode can simultaneously transmit and receive in the same frequency band. Therefore, the wireless channel between two full-duplex nodes can be bidirectional, having the potential to double the spectral efficiency when compared to the half-duplex network. Due to the proximity of the transmit and receive antennas on a node, the overwhelming self-interference becomes the fundamental challenge in implementing a full-duplex network. The mitigation of the

self-interference signal can be managed at each step of the communication network by passive and active cancellation methods [1]. In recent work [2–4], the feasibility of the single input single output (SISO) full-duplex communication has been experimentally demonstrated. However, the performance is limited by the residual self-interference which is considered in [1, 4–6] to be induced by the imperfection of the transmit front-end chain.

The performance bottleneck from imperfect transmit front-end chain has motivated recent research in full-duplex channel with transmit front-end noise. The performance of the SISO full-duplex two-way channel has been thoroughly analyzed in [1, 7]. The multiple input multiple output (MIMO) full-duplex two-way channel with transmit front-end noise is considered in [5, 6, 8] (in [5, 6] termed as MIMO full-duplex bidirectional channel). In [5], the transmit front-end noise was modeled as a white Gaussian noise. Following the transmission noise model, the effect of time-domain cancellation and spatial-domain suppression on a full-duplex channel were studied. In [6], a full-duplex channel was modeled with the transmit front-end noise and under the limited dynamic range. The authors then proposed a numerical method to solve the signaling that maximizes the lower bound of achievable sum-rate for such a full-duplex channel. The maximization of the weighted achievable sum-rate for a full-duplex channel was considered under the imperfect transmit front-end chain in [8].

Within this context, we consider optimally operating a full-duplex channel under imperfect front-end chains. We introduce a full-duplex channel model that includes the effect of imperfect transmit front-end chain and limited transmitter dynamic range. Such a channel model is closely related to a Gaussian interference channel model, which were widely studied in [9–11]. Inspired by the work in [9–11], we consider a full-duplex two-way channel in a game-theoretical framework. Consequently, we characterize a full-duplex channel by Pareto boundary and Nash equilibrium. In game theory, Pareto boundary is a definition with the global optimality whereas Nash equilibrium is with the competitive optimality. Unlike the global optimality, competitive optimality is a definition of optimality that can be achieved by distributed algorithms.

For a MIMO full-duplex channel, the Pareto boundary of the achievable rate region is described by a family of non-convex optimization problems. In the special case, where there is only a single receive antenna, we can decouple the original non-convex problems to a family of convex optimization problems [12, 13]. By employing the semi-definite programming (SDP) reformulation, we then numerically solve the Pareto-optimal signaling by which the Pareto boundary of a

MISO full-duplex channel can be achieved. We further prove that the rank of Pareto-optimal signaling is always equal to one. That is to say, for a MISO full-duplex two-way channel, transmit beamforming scheme is capable of achieving the entire Pareto boundary. Furthermore, we propose a closed-form for the optimal beamforming weights.

The Pareto boundary of a general MIMO full-duplex channel cannot be decoupled or transformed into a convex form. It implies that, to find the Pareto boundary, a family of centralized nonconvex problems needs to be solved, which renders the computation intractable. Therefore, for a general MIMO full-duplex channel we restrict our attention to the optimality which can be achieved by fully distributed algorithms. In other words, instead of the Pareto boundary, we aim to achieve the Nash equilibrium for a general MIMO full-duplex channel. In this paper, we first prove the existence of the Nash equilibrium for a MIMO full-duplex channel. We then derive a condition to ensure the uniqueness of Nash equilibrium. The signaling at the Nash equilibrium can be derived by our proposed algorithm, which is modified from the iterative water-filling algorithm (IWFA) in [11].

The rest of the paper is organized as follows. In Section II the channel model for a MIMO two-way full-duplex wireless channel is presented. Section III presents the description of the Pareto optimality and the competitive optimality, which correspond to the Pareto boundary and the Nash equilibrium, respectively. The characterizations of the Pareto boundary and the Nash equilibrium for a full-duplex channel are also provided. In Section IV the Pareto boundary of a MISO full-duplex channel is derived, where the beamforming scheme is proved to be optimal. The closed-form solution for the optimal beamforming weights is then presented. Section V presents the existence of the Nash equilibrium for a full-duplex channel. The condition for the uniqueness of NE is also provided. Here, we propose a modified iterative water-filling algorithm to achieve the NE. Numerical examples are provided in Section VI. While the conclusions are given in Section VII.

Notation: We use $(\cdot)^\dagger$ to denote conjugate transpose. For a scalar a , we use $|a|$ to denote the absolute value of a . For a vector $\mathbf{a} \in \mathbb{C}^{M \times 1}$, we use $\|\mathbf{a}\|$ to denote the norm, $\mathbf{a}^{(k)}$ to denote the k^{th} element of \mathbf{a} , $\text{Diag}(\mathbf{a})$ to denote the square diagonal matrix with the elements of vector \mathbf{a} on the main diagonal. For a matrix $\mathbf{A} \in \mathbb{C}^{M \times M}$, we use \mathbf{A}^{-1} , $\text{tr}(\mathbf{A})$ and $\text{rank}(\mathbf{A})$ to denote the inverse, the trace and the rank of \mathbf{A} , respectively. We use $\text{diag}(\mathbf{A})$ to denote the diagonal matrix with the same diagonal elements as \mathbf{A} . $\mathbf{A} \succeq 0$ means that \mathbf{A} is a positive semidefinite

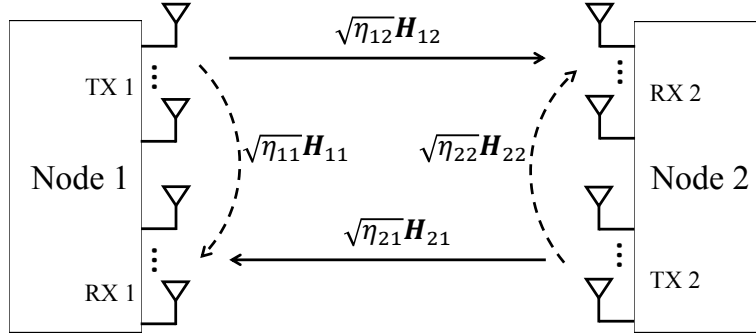


Fig. 1: The MIMO point-to-point full-duplex network under study. The solid lines denote the direct channels and the dashed lines denote the self-interference channels.

Hermitian matrix. We denote expectation, variance and covariance by $E\{\cdot\}$, $\text{Var}\{\cdot\}$ and $\text{Cov}\{\cdot\}$, respectively. Finally, \mathbb{C} and \mathbb{H} denotes the complex field and the Hermitian symmetric space, respectively.

II. CHANNEL MODEL

In this section, we present the channel model for a MIMO full-duplex (FD) network with two nodes as illustrated in Fig. 1. We assume that two nodes indexed by $i, j \in \{1, 2\}$ share the same single frequency band for transmission. Each node has a transmitter and a receiver. The transmitter is equipped with M physical antennas and the receiver with N physical antennas, where each single antenna is connected to a front-end chain. The signal from transmitter i is collected as the signal of interest by receiver $j, j \neq i$, while appears at its own receiver i as the self-interference signal.

As illustrated in Fig. 1 the direct channel between two nodes is denoted by $\sqrt{\eta_{ij}}\mathbf{H}_{ij}, i \neq j$, where η_{ij} represents the average power gain of the direct channel. Similarly, the self-interference channel within each node is characterized by the channel matrix \mathbf{H}_{ii} and the average power gain η_{ii} . According to [6], all the channels in the above full-duplex network can be modeled as the Rayleigh fading channel. That is, all channel matrices are with i.i.d complex Gaussian entries with zero mean and unit variance. We define $\gamma_i \triangleq \frac{\eta_{ji}}{\eta_{ii}}$ to represent the relative strength of the direct channel and the self-interference channel.

While passing through the transmit front-end chain, the intended transmit signal is corrupted by distortions in the power amplifier, non-linearities in the DAC and phase noise [4, 5]. The

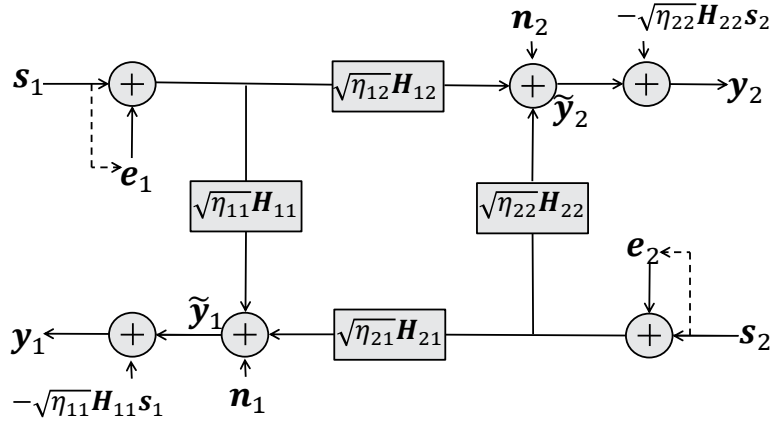


Fig. 2: The MIMO point-to-point full-duplex network under study. The solid line denotes the desired channel and the dashed line denotes the self-interference channel.

results in [4, 5] demonstrate that all the impairments induced by the imperfect front-end chain can be comprehensively modeled by an additive Gaussian noise, namely, the transmit front-end noise. Furthermore, the power of the transmit front-end noise is β times proportional to that of the intended transmit signal due to the limited dynamic range of the transmit front-end chain [4, 6]. Here, β denotes the noise level of the transmit front-end chain [6].

Fig. 2 summarizes our full-duplex channel model. The signal at receiver i is given by

$$\tilde{\mathbf{y}}_i = \sqrt{\eta_{ji}} \mathbf{H}_{ji} (\mathbf{s}_j + \mathbf{e}_j) + \sqrt{\eta_{ii}} \mathbf{H}_{ii} (\mathbf{s}_i + \mathbf{e}_i) + \mathbf{n}_i, \quad (1)$$

where $\mathbf{s}_i \in \mathbb{C}^{M \times 1}$ denotes the intended transmit signal at transmitter i , the channel matrices $\mathbf{H}_{ij} \in \mathbb{C}^{N \times M}$. The transmit front-end noise \mathbf{e}_i is propagated over the same channel as \mathbf{s}_i . Denote the covariance of \mathbf{s}_i by $\mathbf{Q}_i \triangleq \text{Cov}\{\mathbf{s}_i\}$. Note that the m^{th} diagonal element of \mathbf{Q}_i represents the transmit signal power of the m^{th} antenna at transmitter i . Thus, \mathbf{e}_i can be modeled as the Gaussian vector with zero mean and covariance $\text{Cov}\{\mathbf{e}_i\} = \beta \text{diag}(\mathbf{Q}_i)$ [6, 8]. The thermal noise at receiver i is modeled as $\mathbf{n}_i \sim \mathcal{CN}(0, \mathbf{I}_N)$, where \mathbf{I}_N denotes the $N \times N$ identity matrix.

At receiver i , the signal of interest $\mathbf{H}_{ji} \mathbf{s}_j, j \neq i$ is received along with the self-interference signal $\mathbf{H}_{ii} \mathbf{s}_i$ and the transmit front-end noise $\mathbf{H}_{ji} \mathbf{e}_j, \mathbf{H}_{ii} \mathbf{e}_i$. The power level of $\mathbf{H}_{ji} \mathbf{e}_j, j \neq i$ is typically much lower than that of the thermal noise \mathbf{n}_i and thus can be neglected [5]. However, $\mathbf{H}_{ii} \mathbf{e}_i$ is in the power level close to the signal of interest and needs to be considered for analysis, since the power gain of the self-interference channel \mathbf{H}_{ii} overwhelms the power gain of the direct channel \mathbf{H}_{ji} [6].

In addition to the strength, transmitters and receivers on a same node are relatively static, resulting in the long coherence time of self-interference channels, thus receiver i is assumed to have the perfect knowledge of its own self-interference channel \mathbf{H}_{ii} [5]. Note that receiver i also knows its own transmitted signal \mathbf{s}_i . Then we can eliminate the self-interference $\mathbf{H}_{ii}\mathbf{s}_i$ before decoding. The signal after cancellation is given by

$$\mathbf{y}_i = \sqrt{\eta_{ji}}\mathbf{H}_{ji}\mathbf{s}_j + \sqrt{\eta_{ii}}\mathbf{H}_{ii}\mathbf{e}_i + \mathbf{n}_i, \quad (2)$$

where $\mathbf{H}_{ii}\mathbf{e}_i$ represents the residual self-interference.

III. PARETO OPTIMALITY AND COMPETITIVE OPTIMALITY

As shown in (2), the transmission from node j to node i is corrupted by the residual self-interference of node i and the thermal noise. The sum of all such interferences is equal to an additive Gaussian noise \mathbf{v}_i . Let us define Σ_i to be the covariance of \mathbf{v}_i , then $\Sigma_i = \mathbf{I} + \beta\eta_{ii}\mathbf{H}_{ii}\text{diag}(\mathbf{Q}_i)\mathbf{H}_{ii}^\dagger$, which is a function of \mathbf{Q}_i . It follows from the results of [14, 15] that by employing a Gaussian codebook at node 1, we can achieve the maximum rate for the transmission from node 1 to node 2

$$R_1(\mathbf{Q}_1, \mathbf{Q}_2) = \log \det(\mathbf{I} + \eta_{12}\mathbf{H}_{12}^\dagger \Sigma_2^{-1} \mathbf{H}_{12}\mathbf{Q}_1), \quad (3)$$

where $(\mathbf{Q}_1, \mathbf{Q}_2)$ are the transmit covariance matrices of the nodes. Similarly, the maximum rate for the transmission from node 2 to node 1 is equal to

$$R_2(\mathbf{Q}_1, \mathbf{Q}_2) = \log \det(\mathbf{I} + \eta_{21}\mathbf{H}_{21}^\dagger \Sigma_1^{-1} \mathbf{H}_{21}\mathbf{Q}_2). \quad (4)$$

Denote the feasible set of the covariance matrix \mathbf{Q}_i as \mathcal{X}_i . A set of $(\mathbf{Q}_1, \mathbf{Q}_2)$ is feasible if it satisfies the transmit power constraints P_1, P_2 . Thus, we have $\mathcal{X}_i = \{\mathbf{Q}_i \in \mathbb{H}^M | \mathbf{Q}_i \succeq 0, \text{tr}(\mathbf{Q}_i) \leq P_i\}$. Once $(\mathbf{Q}_1, \mathbf{Q}_2)$ are given, only rate pair (r_1, r_2) with $r_1 \leq R_1, r_2 \leq R_2$ is achievable for the FD channel. Thus, the achievable rate region for the MIMO FD two-way channel with the transmit power constraints P_1, P_2 can be described as the following set:

$$\mathcal{R} \triangleq \bigcup_{\substack{\mathbf{Q}_1 \in \mathcal{X}_1, \\ \mathbf{Q}_2 \in \mathcal{X}_2}} \left\{ (r_1, r_2) : \begin{array}{l} 0 \leq r_1 \leq R_1(\mathbf{Q}_1, \mathbf{Q}_2) \\ 0 \leq r_2 \leq R_2(\mathbf{Q}_1, \mathbf{Q}_2) \end{array} \right\}, \quad (5)$$

where R_1 and R_2 in (3) and (4), respectively, are mutually coupled by the covariance matrices \mathbf{Q}_1 and \mathbf{Q}_2 . Therefore, there always exists performance tradeoffs between R_1 and R_2 in a selection of $(\mathbf{Q}_1, \mathbf{Q}_2)$. Such tradeoffs can be considered as a game in which node i is player i , $R_i(\mathbf{Q}_1, \mathbf{Q}_2)$ is the payoff of player i and \mathbf{Q}_i is the admissible strategy of player i . All possible outcomes of the game are characterized in the achievable rate region \mathcal{R} . As a sequence, all concepts of a FD channel can be interpreted from a game-theoretic view. Driven by the global optimality, we first consider the Pareto boundary for a FD two-way channel. The Pareto boundary is characterized by a set of 'jointly' optimal rate pairs (R_1, R_2) . Each jointly optimal rate pair is of the Pareto-optimality, which is defined as follows (A similar definition can be found in [16–18]).

Definition 1 (Pareto optimality). A rate pair $(R_1^*, R_2^*) \in \mathcal{R}$ is Pareto optimal if there does not exist another rate pair $(R_1, R_2) \in \mathcal{R}$ such that $(R_1, R_2) \geq (R_1^*, R_2^*)$ and $(R_1, R_2) \neq (R_1^*, R_2^*)$ where the inequality is component-wise.

The Pareto boundary refers to the outer boundary of the achievable rate region \mathcal{R} in (5). Thus, we can define the Pareto boundary \mathcal{R}^* as follows

$$\mathcal{R}^* = \bigcup \{ \text{all the Pareto optimal rate pairs } (R_1^*, R_2^*) \text{ in } \mathcal{R} \}. \quad (6)$$

Each point on the Pareto boundary \mathcal{R}^* maximizes one of the weighted sum-rates for the FD channel [12, 19]. Therefore, \mathcal{R}^* can be derived by solving a family of weighted sum-rate optimization problems:

$$\begin{aligned} & \max_{\mathbf{Q}_1, \mathbf{Q}_2} \mu_1 R_1(\mathbf{Q}_1, \mathbf{Q}_2) + \mu_2 R_2(\mathbf{Q}_1, \mathbf{Q}_2) \\ & \text{subject to } \mathbf{Q}_i \in \mathcal{X}_i, i = 1, 2, \end{aligned} \quad (7)$$

where $0 \leq \mu_1, \mu_2$ and $\mu_1 + \mu_2 = 1$.

The optimal solutions $(\mathbf{Q}_1^*, \mathbf{Q}_2^*)$ for problem (7) with some μ_1, μ_2 correspond to one pair of Pareto-optimal transmission strategies for the FD channel. To obtain the entire Pareto boundary, we need to derive all Pareto-optimal strategies. However, the centralized non-convex nature of problem (7) poses two serious issues in achieving the Pareto boundary. First, solving the Pareto-optimal strategies in general comes at the price of prohibitively high computationally complexity due to the non-convexity of problem (7). Second, problem (7) is coupled by $\mathbf{Q}_1, \mathbf{Q}_2$. Hence, it requires an extra central node to acquire the full knowledge of the FD channel and then solve the Pareto-optimal strategies. Due to these challenges, it is often not practical to operate a FD

channel in its Pareto optimality. An alternative way is that each node would compete for its own payoff irrespective of the other node's payoff. The optimality built in such a scenario is defined as follows.

Definition 2 (competitive optimality). For a two-way FD channel, \mathcal{X}_i is the nonempty set of all feasible strategies for node i . A strategy profile $(\mathbf{Q}_1^*, \mathbf{Q}_2^*) \in \mathcal{X}_1 \times \mathcal{X}_2$ is competitive optimal if the following condition holds for all $i, j \in \{1, 2\}, i \neq j$:

$$R_i(\mathbf{Q}_i^*, \mathbf{Q}_j^*) \geq R_i(\mathbf{Q}_i, \mathbf{Q}_j^*), \forall \mathbf{Q}_i \in \mathcal{X}_i. \quad (8)$$

If the competitive optimality is achieved, any unilateral change of strategies would result in a rate loss for the FD channel [11]. From the game theoretic view, a set of competitive optimal strategies corresponds to a Nash equilibrium (NE) of the FD channel. To obtain an NE, we construct a non-cooperative game according to Definition 2. In the game, node i is assumed to have the knowledge of the direct channel \mathbf{H}_{ij} and its own self-interference channel \mathbf{H}_{ii} , and have a fixed power budget P_i . At each iteration, given the strategy of node j , node i locally chooses its strategy \mathbf{Q}_i to maximize its pay-off R_i , which can be described by the rate-maximization problem as follows:

$$\begin{aligned} & \max_{\mathbf{Q}_i} R_i(\mathbf{Q}_i, \mathbf{Q}_j) \\ & \text{subject to } \mathbf{Q}_i \in \mathcal{X}_i, \end{aligned} \quad (9)$$

In the non-cooperative game, the optimization problem (9) is repeatedly done by both nodes until an equilibrium is reached, if any.

If deriving the Pareto boundary straight from problem (7), one needs to simultaneously search \mathbf{Q}_1 and \mathbf{Q}_2 in $\mathcal{X}_1 \times \mathcal{X}_2$. In contrast, the non-cooperative game for an NE is in a fully distributed fashion, where each node derives its own \mathbf{Q}_i from \mathcal{X}_i . More important, problem (7) is non-convex while problem (9) is convex. Accordingly, an NE promises much higher computational efficiency than the Pareto boundary. An NE is of the competitive optimality, however, not guaranteed to achieve the Pareto optimality. Therefore, the tradeoff between performance and computational efficiency should be considered in the strategy design for a FD channel.

In the sequel, we will investigate further into the transmission strategy design within the framework of game theory so as to improve the performance of the two-way FD channel. We

will first consider the simple case where each FD node is equipped with single receive antenna, and then consider the general MIMO case.

IV. MISO FULL-DUPLEX CHANNEL

We consider the scenario where all FD nodes are equipped with only one receive antenna i.e., $N = 1$. Consequently, all the channels are reduced to MISO, and can be represented by vectors $\mathbf{h}_{ij}, i, j \in \{1, 2\}$. The maximum rate for the channel from node i to node j can be then simplified as

$$R_i(\mathbf{Q}_i, \mathbf{Q}_j) = \log \left(1 + \frac{\eta_{ij} \mathbf{h}_{ij}^\dagger \mathbf{Q}_i \mathbf{h}_{ij}}{1 + \beta \eta_{jj} \mathbf{h}_{jj}^\dagger \text{diag}(\mathbf{Q}_j) \mathbf{h}_{jj}} \right), \quad (10)$$

where $(\mathbf{Q}_1, \mathbf{Q}_2)$ are the given transmit covariance matrices. In contrast with the general MIMO rates in (3) and (4), the rate for the MISO case in (10) is in a simpler form, which then improves the efficiency in solving the Pareto boundary.

A. Decoupled Optimization Problems

The difficulty in deriving Pareto boundary for the MIMO FD channel is caused by the non-convexity and the coupled high-dimensional nature of problem (7). To render the derivation tractable, we need to decouple problem (7) in terms of lower-dimensional variables. Inspired by the decoupling procedure in [12, 18, 19] we introduce an auxiliary variable z_i to denote the power of the received signal at node j i.e., $z_i \triangleq \mathbf{h}_{ij}^\dagger \mathbf{Q}_i \mathbf{h}_{ij}$. With z_i , we then construct the following optimization problem of \mathbf{Q}_i under the transmit power constraint P_i :

$$\begin{aligned} & \min \mathbf{h}_{ii}^\dagger \text{diag}(\mathbf{Q}_i) \mathbf{h}_{ii} \\ & \text{subject to } \mathbf{h}_{ij}^\dagger \mathbf{Q}_i \mathbf{h}_{ij} = z_i \\ & \mathbf{tr}(\mathbf{Q}_i) \leq P_i, \mathbf{Q}_i \succeq 0 \end{aligned} \quad (11)$$

where $i, j \in \{1, 2\}$ and $i \neq j$. Here, we require

$$0 \leq z_i \leq \max_{\mathbf{Q}_i \in \mathcal{X}_i} \mathbf{h}_{ij}^\dagger \mathbf{Q}_i \mathbf{h}_{ij} = P_i \|\mathbf{h}_{ij}\|^2 \quad (12)$$

so that problem (11) always has a feasible solution. We define $\overline{\mathcal{R}}$ as the set of all optimal solutions for problem (11).

Unlike problem (7) where the objective function is regrading \mathbf{Q}_1 and \mathbf{Q}_2 , problem (11) depends only on \mathbf{Q}_i . In Lemma 1, we show that the Pareto boundary for the MISO FD channel can be alternatively characterized by solving problem (11).

Lemma 1. For a MISO full-duplex channel with the transmit power constraint P_i , any point on the Pareto boundary \mathcal{R}^* for the achievable rate region \mathcal{R} in (5) can be achieved by the optimal solution \mathbf{Q}_i^* for problem (11) with some z_i . That is to say, $\mathcal{R}^* \subseteq \overline{\mathcal{R}}$.

Proof: Denote the optimal value of problem (11) as $\Gamma_i^*(z_i)$. Then, we can define $\overline{\mathcal{R}}$ in terms of z_i and $\Gamma_i^*(z_i)$ as follows:

$$\overline{\mathcal{R}} \triangleq \bigcup_{\substack{z_1 \in [0, P_1 \| \mathbf{h}_{12} \|^2], \\ z_2 \in [0, P_2 \| \mathbf{h}_{21} \|^2]}} \left\{ (r_1, r_2) : \begin{cases} r_1 = \log \left(1 + \frac{\eta_{12} z_2}{1 + \beta \eta_{11} \Gamma_1^*(z_1)} \right) \\ r_2 = \log \left(1 + \frac{\eta_{21} z_1}{1 + \beta \eta_{22} \Gamma_2^*(z_2)} \right) \end{cases} \right\}.$$

For any point (R_1^*, R_2^*) on the Pareto boundary, assume that it is achieved by \mathbf{Q}_1^* and \mathbf{Q}_2^* . \mathbf{Q}_i^* is a feasible solution for problem (11) with $z_i = z_i^* = \mathbf{h}_{ij}^\dagger \mathbf{Q}_i^* \mathbf{h}_{ij}$ where $i, j \in \{1, 2\}$ and $i \neq j$. Let $i = 1$, if \mathbf{Q}_1^* is not an optimal solution for problem (11) i.e., $\mathbf{h}_{11}^\dagger \text{diag}(\mathbf{Q}_1^*) \mathbf{h}_{11} > \Gamma_1^*(z_1^*)$ then

$$R_1^* < \log \left(1 + \frac{\eta_{21} z_2^*}{1 + \beta \eta_{11} \Gamma_1^*(z_1^*)} \right) = \overline{R}_1,$$

while

$$R_2^* \leq \log \left(1 + \frac{\eta_{12} z_1^*}{1 + \beta \eta_{22} \Gamma_2^*(z_2^*)} \right) = \overline{R}_2.$$

As $(\overline{R}_1, \overline{R}_2)$ belongs to $\overline{\mathcal{R}}$ and thus belongs to \mathcal{R} , $R_1^* < \overline{R}_1$ and $R_2^* \leq \overline{R}_2$ contradict to the Pareto optimality of (R_1^*, R_2^*) . Therefore \mathbf{Q}_1^* is an optimal solution for problem (11). In the same way we can show that \mathbf{Q}_2^* is an optimal solution for problem (11). \blacksquare

We stress that the set $\overline{\mathcal{R}}$ is not necessarily equivalent to the Pareto boundary \mathcal{R}^* , since $\overline{\mathcal{R}}$ may include the rate pairs inside the region \mathcal{R} . However, the relationship $\mathcal{R}^* \subseteq \overline{\mathcal{R}}$ implies that any approach of obtaining the set $\overline{\mathcal{R}}$ will suffice to derive the entire Pareto boundary \mathcal{R}^* . Furthermore, any result applying to $\overline{\mathcal{R}}$ also works for \mathcal{R}^* . Hence, we proceed to explore the optimal signaling for the MISO FD two-way channel by the study of the set $\overline{\mathcal{R}}$.

B. Optimal Beamforming

Problem (11) is not a common optimization problem since the objective function includes the non-linear operator $\text{diag}(\cdot)$. By setting $\mathbf{A}_i = \mathbf{h}_{ij}\mathbf{h}_{ij}^\dagger$, $\mathbf{C}_i = \text{Diag}(|\mathbf{h}_{ii}^{(1)}|^2, \dots, |\mathbf{h}_{ii}^{(M)}|^2)$ and using the equivalent relationship $\mathbf{h}_{ii}^\dagger \text{diag}(\mathbf{Q}_i)\mathbf{h}_{ii} = \text{tr}(\mathbf{C}_i\mathbf{Q}_i)$, we reformulate problem (11) to the semi-definite programming (SDP) problem as follows (See more details about SDP in [13]):

$$\begin{aligned} \min_{\mathbf{Q}_i} \quad & \text{tr}(\mathbf{C}_i\mathbf{Q}_i) \\ \text{subject to} \quad & \text{tr}(\mathbf{A}_i\mathbf{Q}_i) = z_i, \mathbf{Q}_i \in \mathcal{X}_i, \end{aligned} \quad (13)$$

where $\mathbf{C}_i, \mathbf{A}_i \in \mathbb{H}^M$. The above SDP reformulation reveals the hidden convexity of problem (11) so that we can solve it by employing the well-developed interior-point algorithm within polynomial time. Furthermore, we can numerically characterize the Pareto boundary for the MISO FD two-way channel in efficiency.

The optimal solutions for problem (13) determine the signaling structure to achieve the rate pairs in the set $\overline{\mathcal{R}}$. In Theorem 1, we explore the rank of optimal solutions \mathbf{Q}_i^* for problem (13) where $i, j \in \{1, 2\}$ and $i \neq j$.

Theorem 1. For problem (13) with $P_i \geq 0$ and $0 \leq z_i \leq P_i\|\mathbf{h}_{ij}\|^2$, there always exists an optimal solution \mathbf{Q}_i^* with $\text{rank}(\mathbf{Q}_i^*) = 1$.

Proof: See Appendix A. ■

Note that the transmit signal with the rank-one covariance matrix can be implemented by transmitter beamforming. It follows from Theorem 1 that all points in the set $\overline{\mathcal{R}}$, which include the entire Pareto boundary, can be achieved by the transmitter beamforming. Therefore, we conclude that transmitter beamforming is an optimal scheme for the MISO FD two-way channel. In Lemma 2 we derive the closed-form of the optimal weights for transmitter beamforming.

Lemma 2. For node i in the MISO point-to point FD wireless network with the transmit power constraint P_i and complex channels $\mathbf{h}_{ii}, \mathbf{h}_{ij}, i, j \in \{1, 2\}, i \neq j$, the optimal beamforming weights have the following form:

$$\mathbf{w}_i^* = \frac{\sqrt{z_i}(\mathbf{C}_i + \epsilon\mathbf{I})^{-1}\mathbf{h}_{ij}}{\mathbf{h}_{ij}^\dagger(\mathbf{C}_i + \epsilon\mathbf{I})^{-1}\mathbf{h}_{ij}} \quad (14)$$

where $\mathbf{C}_i = \text{Diag}(|\mathbf{h}_{ii}^{(1)}|^2, \dots, |\mathbf{h}_{ii}^{(M)}|^2)$, constant z_i is within the range $0 \leq z_i \leq P_i\|\mathbf{h}_{ij}\|^2$ and \mathbf{I} denotes the $M \times M$ identical matrix. For a fixed z_i , nonnegative constant ϵ is adjusted to satisfy

the transmit power constraint $\|\mathbf{w}_i\|^2 \leq P_i$. Specially, $\epsilon = 0$ if

$$z_i \leq \frac{P_i(\mathbf{h}_{ij}^\dagger \mathbf{C}_i^{-1} \mathbf{h}_{ij})^2}{\mathbf{h}_{ij}^\dagger \mathbf{C}_i^{-2} \mathbf{h}_{ij}}. \quad (15)$$

Proof: The optimal beamforming weights can be obtained by solving problem (13) with the rank-one constraint $\mathbf{Q}_i = \mathbf{w}_i \mathbf{w}_i^\dagger$ as follows:

$$\begin{aligned} \min_{\mathbf{w}_i} \quad & \mathbf{w}_i^\dagger \mathbf{C}_i \mathbf{w}_i \\ \text{subject to} \quad & |\mathbf{w}_i^\dagger \mathbf{h}_{ij}|^2 = z_i, \|\mathbf{w}_i\|^2 \leq P_i. \end{aligned} \quad (16)$$

The above problem has the general closed-form optimal solution (14) (see details in [20]). Without the transmit power constraint $\|\mathbf{w}_i\|^2 \leq P_i$, problem (16) has the following optimal solution (shown in [20])

$$\mathbf{w}_i^* = \frac{\sqrt{z_i} \mathbf{C}_i^{-1} \mathbf{h}_{ij}}{\mathbf{h}_{ij}^\dagger \mathbf{C}_i^{-1} \mathbf{h}_{ij}}. \quad (17)$$

Combining (17) and the condition (15),

$$\|\mathbf{w}_i^*\|^2 = \frac{z_i \mathbf{h}_{ij}^\dagger \mathbf{C}_i^{-2} \mathbf{h}_{ij}}{(\mathbf{h}_{ij}^\dagger \mathbf{C}_i^{-1} \mathbf{h}_{ij})^2} \leq P_i.$$

Hence, we conclude that $\epsilon = 0$ under the condition (15). ■

We remark that the optimal beamforming weights for node i is closely parallel to the direct channel \mathbf{h}_{ij} , beamforming the signal of interest at node j . While the transmit front-end noise corresponding to the stronger self-interference channel is largely suppressed via the matrix $(\mathbf{C}_i + \epsilon \mathbf{I})^{-1}$.

V. MIMO FULL-DUPLEX CHANNEL

In the MIMO full-duplex network, i.e., $M > 1$ and $N > 1$, there is in general no approach to decouple and convexify problem (7). To characterize the Pareto boundary, one needs to solve problem (7) for all possible weights (μ_1, μ_2) . For each pair (μ_1, μ_2) , the optimal solutions for problem (7) can be obtained by an exhaustive search over $(\mathbf{Q}_1, \mathbf{Q}_2)$. But the computational complexity of the exhaustive search is prohibitively high since the search is coupled by high-dimensional \mathbf{Q}_1 and \mathbf{Q}_2 . In [6], the numerical methods, such as Gradient Projection, are used to improve the computational efficiency. However, any numerical method can not be guaranteed to find the global optimum due to the non-convexity of problem (7). In addition, problem (7)

can not be decoupled, implying that an extra central node is required to solve the Pareto-optimal solutions. The central node needs to have full knowledge of the FD network, which poses an extra difficulty in the implementation of a FD channel. Consequently, for the general MIMO FD channel we restrict our attention to the non-cooperative game, by which the FD channel can be operated in its competitive optimality. Such a game is convex and in a fully distributed fashion, rendering the computation tractable. At each iteration of the game, node i selfishly optimizes its own performance by changing its transmit strategy \mathbf{Q}_i . The objective is to achieve the Nash equilibrium, where each node's transmit strategy is a best response to the other node's strategy.

A. Existence of Nash Equilibrium

To obtain the Nash equilibrium (NE) for a FD channel, node i needs to maximize its rate R_i by solving problem (9). The feasible set of problem (9) is $\mathcal{X}_i = \{\mathbf{Q}_i \in \mathbb{H}^2 | \mathbf{Q}_i \succeq 0, \mathbf{tr}(\mathbf{Q}_i) \leq P_i\}$. We denote the optimal solution of problem (9) as $\mathcal{B}_i(\mathbf{Q}_j)$, where $\mathcal{B}_i(\cdot)$ is a function of \mathbf{Q}_j and $\mathcal{B}_i(\cdot) : \mathcal{X}_j \mapsto \mathcal{X}_i$. If \mathbf{Q}_j is given, then $\mathcal{B}_i(\mathbf{Q}_j)$ satisfies

$$R_i(\mathcal{B}_i(\mathbf{Q}_j), \mathbf{Q}_j) \geq R_i(\mathbf{Q}_i, \mathbf{Q}_j), \forall \mathbf{Q}_i \in \mathcal{X}_i. \quad (18)$$

Thus, $\mathcal{B}_i(\cdot)$ is called *Best-Response* function [11]. We then construct a mapping Φ from the *Best-Response* function $\mathcal{B}_i(\cdot)$:

$$\Phi(\mathbf{Q}_1, \mathbf{Q}_2) = (\mathcal{B}_1(\mathbf{Q}_2), \mathcal{B}_2(\mathbf{Q}_1)), \quad (19)$$

where $\Phi : \mathcal{X}_1 \times \mathcal{X}_2 \mapsto \mathcal{X}_1 \times \mathcal{X}_2$. The input and output of Φ are two sets of feasible transmission strategies for the FD channel, where the output strategy for node i is the best response to the input strategy for node j . At the fixed point of Φ , the input strategies are equal to the output strategies

$$(\mathbf{Q}_1, \mathbf{Q}_2) = \Phi(\mathbf{Q}_1, \mathbf{Q}_2). \quad (20)$$

It follows from (18) and (19) that the competitive optimality in Definition (2) is achieved at the fixed point. Hence, for a FD channel, a NE is equivalent to a fixed-point of the mapping Φ . It follows that the NE can be achieved for the FD channel by deriving the fixed-point of the mapping Φ in (19).

Unlike the Pareto boundary, which is the outer bound of the achievable rate region and thus always exists, the existence of Nash equilibrium is not obvious. In Lemma 3, we prove that a

FD channel always has a Nash equilibrium, regardless of transmit power constraints and channel realizations.

Lemma 3 (Existence of NE). There always exists at least one Nash equilibrium for any MIMO two-way full-duplex channel. That is, the mapping Φ in (19) has at least one fixed point.

Proof: See Appendix C. ■

Lemma 3 illustrates that any FD channel has at least one Nash equilibrium. Thus, it demonstrates that the NE can be considered as an applicable performance metric for MIMO FD two-way channels.

B. Uniqueness of Nash Equilibrium

Unlike the Pareto boundary having infinitely many points, a FD channel need not necessarily have multiple Nash equilibria. One example is the MISO FD channel. In the MISO case, the Nash equilibrium is achieved by the beamforming matrix $\mathbf{Q}_i^{NE} = \mathbf{w}_i \mathbf{w}_i^\dagger$, where $\mathbf{w}_i = \frac{\sqrt{P_i} \mathbf{h}_{ij}}{\mathbf{h}_{ij}^\dagger \mathbf{h}_{ij}}$. Note that $(\mathbf{Q}_1^{NE}, \mathbf{Q}_2^{NE})$ depend only on the channel matrices and transmit power constraints, implying that the Nash equilibrium is unique for the MISO FD channel. It is then natural to ask conditions to guarantee the uniqueness of Nash equilibrium in a general MIMO FD channel. We denote the rank of matrix \mathbf{H}_{ij} as r_{ij} i.e., $r_{ij} \triangleq \text{rank}(\mathbf{H}_{ij})$. Thus we have $r_{ij} \leq \min(M, N)$. We start by assuming the direct channel matrices $\{\mathbf{H}_{ij}\}_{i,j \in \{1,2\}, i \neq j}$ are full row-rank matrices i.e., $r_{ij} = N$. In this scenario, the following Lemma 4 offers the sufficient conditions to ensure the uniqueness of NE for the FD channel.

Lemma 4. Assume the direct channel matrices $\{\mathbf{H}_{ij}\}_{i,j \in \{1,2\}, i \neq j}$ are with full row rank. The full-duplex channel is ensured to have a unique Nash equilibrium if

$$\rho \left(\mathbf{H}_{11}^\dagger \mathbf{H}_{21}^{-\dagger} \mathbf{H}_{21}^{-1} \mathbf{H}_{11} \right) \rho \left(\mathbf{H}_{22}^\dagger \mathbf{H}_{12}^{-\dagger} \mathbf{H}_{12}^{-1} \mathbf{H}_{22} \right) < \frac{\gamma_1 \gamma_2}{\beta^2}, \quad (21)$$

where $\rho(\mathbf{X})$ denotes the spectral radius of the matrix \mathbf{X} .

Proof: See Appendix D. ■

To give the additional physical interpretation of Lemma 4, assume $\mathcal{C}(x)$ to be the cumulative distribution function (cdf) of $\rho \left(\mathbf{H}_{11}^\dagger \mathbf{H}_{21}^{-\dagger} \mathbf{H}_{21}^{-1} \mathbf{H}_{11} \right) \rho \left(\mathbf{H}_{22}^\dagger \mathbf{H}_{12}^{-\dagger} \mathbf{H}_{12}^{-1} \mathbf{H}_{22} \right)$. Following Lemma 4, the Nash equilibrium is guaranteed to be unique with probability $\mathcal{C}(\eta_{21} \eta_{12} / \beta^2 \eta_{11} \eta_{22})$. Due to the non-decreasing property of cdf, $\mathcal{C}(\eta_{21} \eta_{12} / \beta^2 \eta_{11} \eta_{22})$ increases as η_{21}, η_{12} increases, or

$\beta, \eta_{11}, \eta_{22}$ decreases. Note that for a FD channel η_{21}, η_{12} represent the power gains of the direct channels, whereas the strength of the residual self-interference is determined by $\beta, \eta_{11}, \eta_{22}$. Thus, one can increase the probability that the FD channel has a unique Nash equilibrium by improving the direct channel gain or suppressing the residual self-interference.

In Lemma 4, the uniqueness of NE is guaranteed by the contractive property of the mapping Φ with respect to the weighted-maximum norm. However, without the full-rank assumption in the above lemma, the contractive property may not hold for the mapping Φ even if condition (21) is satisfied. As an example, consider a symmetric FD channel with $P_1 = P_2 = 10$, $\beta\eta_{11}/\eta_{21} = \beta\eta_{22}/\eta_{12} = 1$, where the channel matrices are set as

$$\mathbf{H}_{11} = \mathbf{H}_{22} = \begin{bmatrix} -0.1440 + 0.3203i & -0.6735 - 0.0040i \\ -0.4009 + 0.5149i & -0.0351 + 0.6118i \\ 1.3155 + 0.5694i & -1.2339 - 0.4902i \end{bmatrix} \quad (22)$$

$$\mathbf{H}_{12} = \mathbf{H}_{21} = \begin{bmatrix} 1.1187 + 0.8794i & 1.0068 - 0.0645i \\ 0.1281 - 0.3943i & 0.8477 + 0.3248i \\ 1.5970 + 0.2708i & -0.3452 + 2.3450i \end{bmatrix}. \quad (23)$$

Note that the mapping Φ is a contraction with respect to the weighted-maximum norm only if there exists some $\mathbf{w} = [w_1, w_2] > 0$ such that

$$\begin{aligned} \left\| \Phi(\mathbf{Q}_1^{(1)}, \mathbf{Q}_2^{(1)}) - \Phi(\mathbf{Q}_1^{(2)}, \mathbf{Q}_2^{(2)}) \right\|_F^{\mathbf{w}} &< \left\| (\mathbf{Q}_1^{(1)}, \mathbf{Q}_2^{(1)}) - (\mathbf{Q}_1^{(2)}, \mathbf{Q}_2^{(2)}) \right\|_F^{\mathbf{w}}, \\ \forall \mathbf{Q}_1 \in \mathcal{X}_1, \mathbf{Q}_2 \in \mathcal{X}_2, \end{aligned} \quad (24)$$

where $\mathcal{X}_i = \{\mathbf{Q} \in \mathbb{H}^2 \mid \mathbf{Q} \succeq 0, \text{tr}(\mathbf{Q}) \leq 10\}$. Let

$$\mathbf{Q}_1^{(1)} = \mathbf{Q}_1^{(2)} = \begin{bmatrix} 0.2208 & 0 \\ 0 & 9.7792 \end{bmatrix} \quad (25)$$

$$\mathbf{Q}_2^{(1)} = \mathbf{Q}_2^{(2)} = \begin{bmatrix} 0.4832 & 0 \\ 0 & 9.5168 \end{bmatrix}. \quad (26)$$

The above set up leads to $\left\| \Phi(\mathbf{Q}_1^{(1)}, \mathbf{Q}_2^{(1)}) - \Phi(\mathbf{Q}_1^{(2)}, \mathbf{Q}_2^{(2)}) \right\|_F^{\mathbf{w}} = 0.1804/\min(w_1, w_2)$ and $\left\| (\mathbf{Q}_1^{(1)}, \mathbf{Q}_2^{(1)}) - (\mathbf{Q}_1^{(2)}, \mathbf{Q}_2^{(2)}) \right\|_F^{\mathbf{w}} = 0.1728/\min(w_1, w_2)$, implying that condition (24) is not satisfied for any $\mathbf{w} = [w_1, w_2] > 0$. Hence, the mapping Φ is not a contraction. However, $\rho(\mathbf{H}_{11}^\dagger \mathbf{H}_{21}^{-\dagger} \mathbf{H}_{21}^{-1} \mathbf{H}_{11}) = 0.4657 < 1$ and $\rho(\mathbf{H}_{22}^\dagger \mathbf{H}_{12}^{-\dagger} \mathbf{H}_{12}^{-1} \mathbf{H}_{22}) = 0.4657 < 1$, so condition

(21) is satisfied. The example therefore demonstrates that Lemma 4 is not true without the full row-rank constraints on $\mathbf{H}_{12}, \mathbf{H}_{21}$. To extent the contractive property of the mapping Φ to all FD channels, stronger conditions are needed. In Theorem 2, we derive the sufficient condition for a general FD channel to have a unique NE.

Theorem 2. A full-duplex channel has a unique NE if $\alpha_1\alpha_2 < 1$, where α_i is defined as

$$\alpha_i \triangleq \begin{cases} \frac{\beta}{\gamma_i} \rho \left(\mathbf{H}_{ii}^\dagger \mathbf{H}_{ji}^{-\dagger} \mathbf{H}_{ji}^{-1} \mathbf{H}_{ii} \right), & \text{if } \text{rank}(\mathbf{H}_{ji}) = N, \\ \frac{\beta}{\gamma_i} \left(1 + \beta \eta_{ii} P_i \rho \left(\mathbf{H}_{ii}^\dagger \mathbf{H}_{ii} \right) \right) \rho \left(\mathbf{H}_{ii}^\dagger \mathbf{H}_{ii} \right) \rho \left(\mathbf{H}_{ji}^{-\dagger} \mathbf{H}_{ji}^{-1} \right), & \text{otherwise.} \end{cases} \quad (27)$$

Proof: See Appendix E. ■

Using the inequality $\rho(\mathbf{A}^\dagger \mathbf{X} \mathbf{A}) \leq \rho(\mathbf{A}^\dagger \mathbf{Y} \mathbf{A})$, where $\mathbf{Y} \succeq \mathbf{X} \succeq 0$, we can obtain

$$\rho \left(\mathbf{H}_{ii}^\dagger \mathbf{H}_{ji}^{-\dagger} \mathbf{H}_{ji}^{-1} \mathbf{H}_{ii} \right) \leq \rho \left(\mathbf{H}_{ii}^\dagger \mathbf{H}_{ii} \right) \rho \left(\mathbf{H}_{ji}^{-\dagger} \mathbf{H}_{ji}^{-1} \right) \quad (28)$$

$$\leq \left(1 + \beta \eta_{ii} P_i \rho \left(\mathbf{H}_{ii}^\dagger \mathbf{H}_{ii} \right) \right) \rho \left(\mathbf{H}_{ii}^\dagger \mathbf{H}_{ii} \right) \rho \left(\mathbf{H}_{ji}^{-\dagger} \mathbf{H}_{ji}^{-1} \right). \quad (29)$$

The above equality demonstrates that the condition in Theorem (2) is stronger than the condition in Lemma (4).

Theorem 2 can be interpreted from two perspectives. On the one hand, assume that the channel matrices are given, Theorem 2 then imposes constraints on $\beta, \eta_{ij}, \eta_{ii}$ to ensure the unique Nash equilibrium for the FD channel. In the case that the direct channel gain η_{ij} is also fixed, $\alpha_1\alpha_2 < 1$ then indicates how small the residual self-interference must be to guarantee the uniqueness of Nash equilibrium. On the other hand, if $\beta, \eta_{jj}, \eta_{ij}$ are given, Theorem 2 then determines the probability that the FD channel is guaranteed to have a unique Nash equilibrium. In the following Corollary 1, we discuss a special FD channel, where all channel matrices $\{\mathbf{H}_{ij}\}_{i,j \in \{1,2\}}$ are circulant. In such a case, Theorem 2 can be further simplified.

Corollary 1. Assume that all the matrices $\{\mathbf{H}_{ij}\}_{i,j \in \{1,2\}}$ have circulant structures. The full-duplex channel is ensured to have a unique Nash equilibrium if

$$\max_{k=1, \dots, M} \frac{|\sigma_{11}(k)|^2}{|\sigma_{21}(k)|^2} \cdot \max_{k=1, \dots, M} \frac{|\sigma_{22}(k)|^2}{|\sigma_{12}(k)|^2} < \frac{\gamma_1 \gamma_2}{\beta^2}, \quad (30)$$

where $\sigma_{ij}(k)$ represents the k^{th} eigenvalue of \mathbf{H}_{ij} . Moreover, $\{|\sigma_{ij}(k)|\}_{k=1}^M$ are i.i.d. Rayleigh random variables with variance M .

The above Corollary implies that a circulant FD channel has a unique Nash equilibrium with probability $P \left(\max_{k=1,\dots,M} \frac{|\sigma_{11}(k)|^2}{|\sigma_{21}(k)|^2} \cdot \max_{k=1,\dots,M} \frac{|\sigma_{22}(k)|^2}{|\sigma_{12}(k)|^2} < \frac{\gamma_1 \gamma_2}{\beta^2} \right)$. Furthermore, the analytical form of the probability P can be derived if the channel matrices are symmetric i.e., $\mathbf{H}_{12} = \mathbf{H}_{21}$ and $\mathbf{H}_{11} = \mathbf{H}_{22}$, $\gamma_1 = \gamma_2 = \gamma$. For the notational convenience, denote $\Gamma(x)$ as the cdf of the ratio A/B , where A and B are two independent Rayleigh random variables. The analytical expression of $\Gamma(x)$ can be found in [21]. Note that $\{\sigma_{ij}(k)\}_{k=1}^M$ are independent Rayleigh random variables. It follows that $\{|\sigma_{ii}(k)|/|\sigma_{ji}(k)|\}_{k=1}^M$ are independently distributed with cdf $\Gamma(x)$. Under the symmetric channel assumption, the probability P thus can be written in terms of $\Gamma(x)$, as follows.

$$P \left(\max_{k=1,\dots,M} \frac{|\sigma_{11}(k)|^2}{|\sigma_{21}(k)|^2} \cdot \max_{k=1,\dots,M} \frac{|\sigma_{22}(k)|^2}{|\sigma_{12}(k)|^2} < \frac{\gamma_1 \gamma_2}{\beta^2} \right) \quad (31)$$

$$= P \left(\max_{k=1,\dots,M} \frac{|\sigma_{11}(k)|}{|\sigma_{21}(k)|} < \sqrt{\frac{\gamma}{\beta}} \right) \quad (32)$$

$$= \prod_{k=1}^M P \left(\frac{|\sigma_{11}(k)|}{|\sigma_{21}(k)|} < \sqrt{\frac{\gamma}{\beta}} \right) = \Gamma^M \left(\sqrt{\frac{\gamma}{\beta}} \right). \quad (33)$$

C. Iterative Water-filling Algorithms

For a given FD channel, we would like to find the transmit covariance matrices $(\mathbf{Q}_1, \mathbf{Q}_2)$ that achieve the NE under transmit power constraints. Following (20), it is equivalent to obtain a fixed-point for the mapping Φ in (19).

We operate a non-cooperative game to obtain the NE for a FD channel. In the game, the transmission strategies are iteratively updated by the mapping Φ in (19). That is, node i changes its strategy as $\mathcal{B}_i(\mathbf{Q}_j)$ at each iteration of update. Note that $\mathcal{B}_i(\mathbf{Q}_j)$ can be easily obtained by applying the water-filling algorithm to problem (9) [11]. Such a non-cooperative game is equivalent to implement the iterative water-filling algorithm (IWFA) in a fully distributed fashion [10, 22]. We first assume that the IWFA is synchronous. That means, all nodes adjust their transmit covariance matrices simultaneously. Then, the transmission strategies at the k^{th} iteration can be written in terms of the strategies at the $(k-1)^{\text{th}}$ iteration,

$$(\mathbf{Q}_1^{(k)}, \mathbf{Q}_2^{(k)}) = \Phi(\mathbf{Q}_1^{(k-1)}, \mathbf{Q}_2^{(k-1)}). \quad (34)$$

Ideally, the IWFA converges to a Nash equilibrium at the l^{th} iteration if the condition $(\mathbf{Q}_1^{(l)}, \mathbf{Q}_2^{(l)}) = \Phi(\mathbf{Q}_1^{(l)}, \mathbf{Q}_2^{(l)})$ is satisfied. In practice, however, we set the tolerance as a small positive number

δ . The stopping criterion of the IWFA is then described as

$$\|\Phi(\mathbf{Q}_1^{(l)}, \mathbf{Q}_2^{(l)}) - (\mathbf{Q}_1^{(l)}, \mathbf{Q}_2^{(l)})\|_F < \delta. \quad (35)$$

To deploy the synchronous IWFA, the synchronization for all nodes is required, which poses an extra issue in the implementation of a FD channel. In an enabled FD channel, the synchronization may not be available. The nodes may delay some updates and even miss some updates. Thus, in order to be robust in such case, we propose an asynchronous version of the IWFA. To describe the possible missing updates, we denote the strategies at k^{th} iteration as $(\mathbf{Q}_1^{\tau(k)}, \mathbf{Q}_2^{\tau(k)})$, where

$$\mathbf{Q}_i^{\tau(k)} = \begin{cases} \mathcal{B}_i(\mathbf{Q}_j^{\tau(k-1)}), & \text{if update at } k^{\text{th}} \text{ iteration is succeeding,} \\ \mathbf{Q}_i^{\tau(k-1)}, & \text{if update at } k^{\text{th}} \text{ iteration is missing,} \end{cases} \quad (36)$$

where $0 \leq \tau(k) \leq k$. The asynchronous IWFA has the following stopping rule,

$$\left\| \left(\mathbf{Q}_1^{\tau(k)}, \mathbf{Q}_2^{\tau(k)} \right) - \left(\mathbf{Q}_1^{\tau(k-1)}, \mathbf{Q}_2^{\tau(k-1)} \right) \right\|_F < \delta. \quad (37)$$

To investigate the convergence of IWFA in a FD channel, we only need to consider the asynchronous IWFA. Since the synchronous IWFA is a special case of the asynchronous IWFA, where $\tau(k) = k, \forall k$. In Lemma 5, the sufficient condition for the convergence of the asynchronous IWFA is derived.

Lemma 5. If a full-duplex channel satisfies the condition (27) in Theorem (2), then the asynchronous IWFA can converge to the unique NE from any initially feasible transmit strategies $(\mathbf{Q}_1^{(0)}, \mathbf{Q}_2^{(0)})$.

Proof: The condition in Theorem 2 guarantees the mapping Φ in (19) to be a contraction with respect to the weighted-maximum norm. It then follows from Proposition 2 that the FD channel has a unique Nash equilibrium. Further, the contractive property w.r.t. $\|\cdot\|_F^w$ can be used to guarantee the asynchronous convergence. See the details of the proof in [23]. ■

It follows from Lemma 5 that the global convergence of the asynchronous IWFA is regardless of the initial point. It implies that the unique NE solved by the asynchronous IWFA is globally asymptotically stable [22] if the FD channel satisfies the condition in Theorem 2.

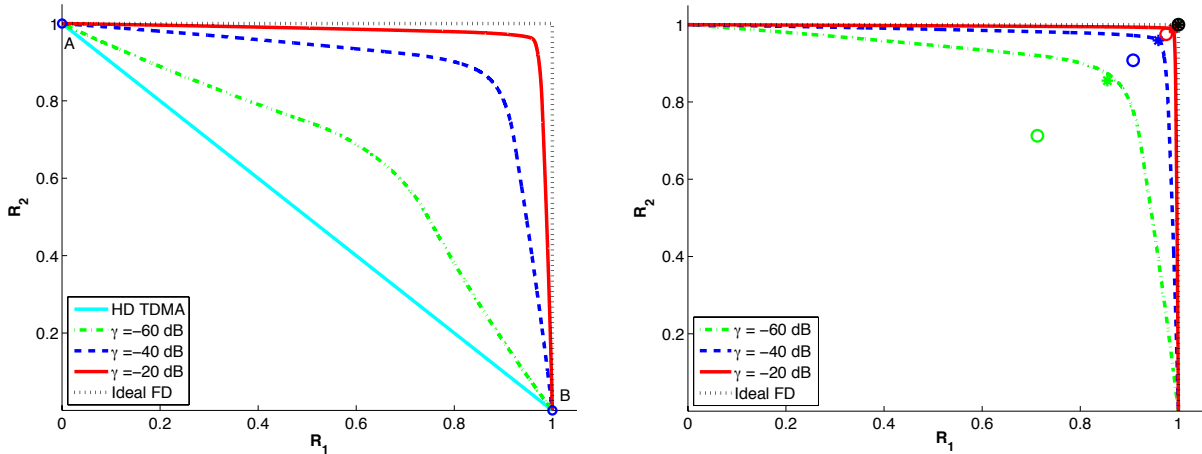
VI. NUMERICAL RESULTS

A. Performance of MISO Full-Duplex Channel

We present the achievable rate regions for the MISO full-duplex two-way channels in Fig. 3a, where the channels are symmetric i.e., $\mathbf{h}_{12} = \mathbf{h}_{21}$ and $\mathbf{h}_{11} = \mathbf{h}_{22}$, $\eta_{11} = \eta_{22}$ and $\eta_{12} = \eta_{21}$. Each node is equipped with $M = 3$ transmit antennas and single receive antenna with the transmit power constraints $P_1 = P_2 = 1$. And we have $\gamma_i = \eta_{ji} - \eta_{ii}$ (in dB). Here we have $\gamma_1 = \gamma_2$ due to the assumption of symmetry. For the notational convenience, we use γ to replace γ_i in the sequel. Note that the self-interference channel gain η_{ii} can be reduced by the passive suppression [3], which leads to an increase of γ . The transmit front-end noise level is fixed with $\beta = -40$ dB, where β is determined by the impairments of the transmit front-end chain. With the analog and digital techniques in [1, 7], such impairments can be partly compensated so that β can be reduced. In Fig. 3, each colored line represents the Pareto boundary of the achievable rate region for the channel with corresponding γ . We conclude from the numerical results that the achievable rate region shrinks as γ varies from -20 dB to -60 dB. However, the FD channel always outperforms than the half-duplex TDMA channel if the optimal beamforming is employed. The extreme points A, B of the rate regions on the axes represent the maximum rates in the case that only one-way of the two-way channel is working. It follows that the points A, B are only determined by the transmit power constraints P_i . The ideal MISO FD two-way channel sets the outer bound for the achievable rate regions of all channels, doubling that of the half-duplex TDMA channel.

In Fig. 3b, we evaluate the Pareto-boundary of the same FD channels as in Fig. 3a but with $\beta = -60$ dB. Comparing the channel with the same γ in Fig. 3a and Fig. 3b, we illustrate that the achievable rate region is increased due to reduction of β . The stars in Fig. 3b represent the Nash equilibria for the FD channels. It can be observed that the Nash equilibrium is not Pareto-optimal except for an ideal FD channel. The circles denote the rate pairs achieved by ZF beamforming. Note that the circles are below the corresponding Nash equilibria except for the ideal FD channel. Thus, we conclude that the Nash equilibrium outperforms than the ZF beamforming for a MISO FD channel in presence of the residual self-interference.

In Fig. 4a, we geometrically compare the optimal beamforming weights, the NE and the zero-forcing beamforming weights. For simplicity, we assume all channels to be 2×1 real-



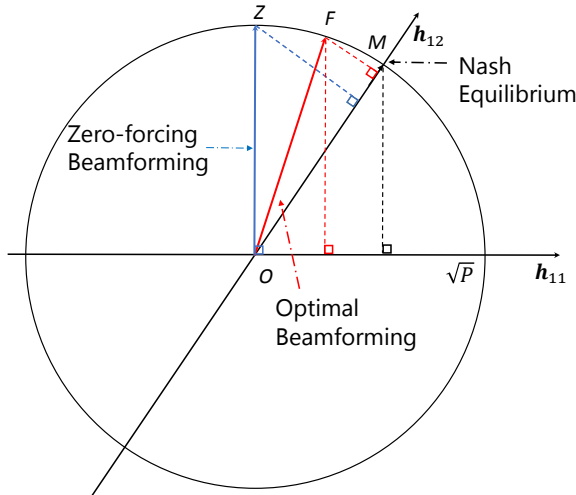
(a) The achievable rate regions for the symmetric MISO FD two-way channels with $\beta = -40$ dB, $\|\mathbf{h}_{12}\| = \|\mathbf{h}_{21}\| = 1$, $P_1 = P_2 = 1$. As plotted for comparison is the half-duplex TDMA achievable rate region.

(b) The achievable rate regions for the symmetric MISO two-way FD channel with $\beta = -60$ dB, $\|\mathbf{h}_{12}\| = \|\mathbf{h}_{21}\| = 1$, $P_1 = P_2 = 1$. Circles denote the ZF beamforming rates. Stars denote the NE.

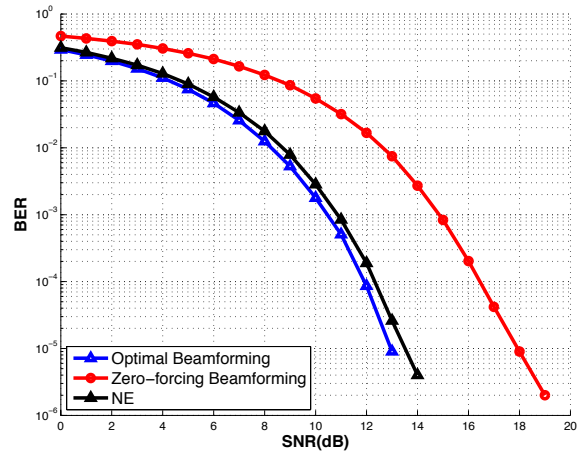
Fig. 3: The comparison of the FD optimal beamforming, the Nash equilibrium and the zero-forcing beamforming

value vectors. We further assume the channels to be symmetric i.e., $\mathbf{h}_{11} = \mathbf{h}_{22}$ and $\mathbf{h}_{12} = \mathbf{h}_{21}$. Assume the transmit power constraints $P_1 = P_2 = P$. Then all possible beamforming weights are contained in the disc with radius \sqrt{P} . In Fig. 4a, \overline{OF} represents the optimal beamforming weights by which the rate pair with maximum sum-rate can be achieved. The zero-forcing (ZF) beamforming weights is represented by \overline{OZ} . Note that \overline{OZ} restricts the transmit signal orthogonal to the self-interference channel \mathbf{h}_{ii} . Compared with the ZF beamforming weights, the optimal \overline{OF} is not orthogonal to \mathbf{h}_{ii} but has greater length of projection on the direct channel \mathbf{h}_{ij} . Among all the weights, the Nash equilibrium \overline{OM} has the greatest length of projection on \mathbf{h}_{ij} . However, the Nash equilibrium is outperformed by the optimal beamforming weights due to the larger amount of self-interference generated by \overline{OM} than \overline{OF} . We remark that the direction of NE coincides with that of the direct channel \mathbf{h}_{ij} in the MISO case. However, it is not true for a general MIMO FD channel.

The achievable rate region shown in Fig. 3b can be achieved only if the infinite-length Gaussian codebook is employed by all nodes. However, the communication systems in practice always choose the discrete-alphabet modulation schemes, such as QPSK or QAM. In Fig. 4b, we show



(a) The geometric comparison of the full-duplex optimal beamforming, the Nash equilibrium and the zero-forcing beamforming.



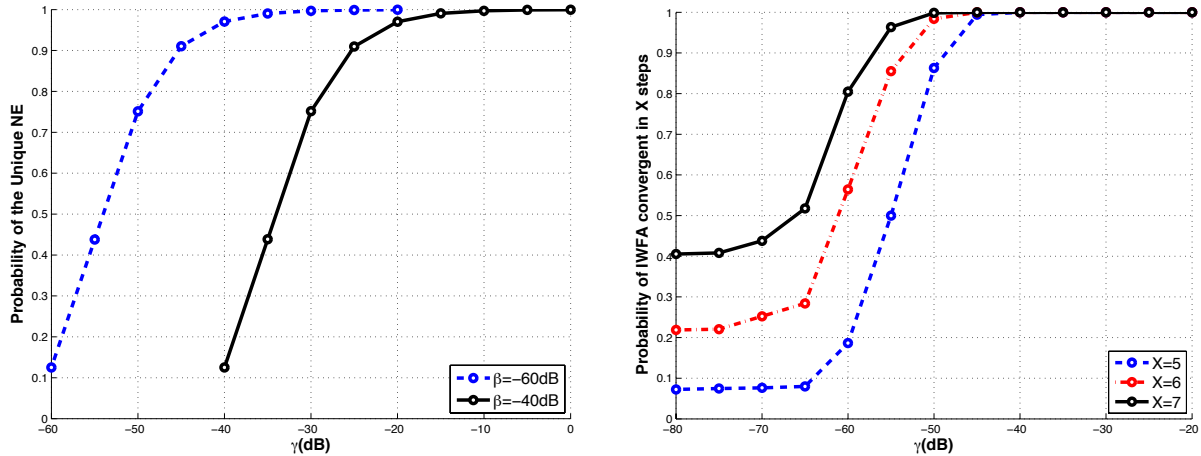
(b) The bit error rate of a symmetric full-duplex QPSK system. Here, $M = 3$, $N = 1$, $P = 1$, $\beta = -60$ dB, $\gamma = -40$ dB.

Fig. 4

the error rate performance for one of the MISO FD channels in Fig. 3b, where γ is equal to -40 dB. We choose QPSK as the modulation scheme and employ the optimal beamforming, Nash equilibrium and zero-forcing beamforming for the FD channel respectively. Note that the FD channel is chosen to be symmetric, implying that the transmission from node 1 to node 2 has the same bit error rate as the transmission from node 2 to node 1. Therefore, we only show the BER performance for one directional transmission.

B. Performance of MIMO Full-Duplex Nash Equilibrium

It follows from Theorem 2 that the uniqueness of NE depends on the channel realizations $\{\mathbf{H}_{ij}\}_{i,j \in \{1,2\}}$. With given β , η_{ij} and η_{ii} , Theorem 2 then gives the probability that NE is guaranteed to be unique. Specially, for a symmetric circulant FD channel, the probability derived from Theorem 2 can be analytically expressed in (33). In Fig. 5a, we plot the probability in (33) as a function of $\gamma = \gamma_1 = \gamma_2$. It follows from Lemma 5 that the condition in Theorem 2 suffices to guarantee the convergence of asynchronous IWFA. Accordingly, Fig. 5a is an analytical lower bound for the probability that IWFA can asynchronously converge to a NE. Moreover, the unique NE is globally asymptotically stable if the condition in Theorem 2 is satisfied. Thus, the larger probability implies that the FD NE is more stable. Accordingly, Fig. 5a indicates the stability



(a) Probability (lower bound) that a FD channel has the unique NE for $\beta = -40$ dB, $\beta = -60$ dB. Here, $M = N = 3$. The channel has a circulant symmetric structure.

(b) Probability that the iterative water-filling algorithm converges to a Nash equilibrium in X steps. Here, $M = N = 3$, $\beta = -60$ dB.

Fig. 5: The performance of the synchronous IWFA

of operating a FD network at its NE.

As illustrated in Fig.5a, the probability in (33) can be increased by either reducing β or increasing γ . For simplicity, assume the direct channel gain is fixed. Then both the reduction of β and the increase of γ lead to the mitigation in residual self-interference. It implies that, for a FD channel, the stability of its competitive optimal strategies can be improved by mitigating the residual self-interference.

In Fig. 5b, we evaluate the computational efficiency of the synchronous iterative water-filling algorithm as a function of γ . We randomly produce 100,000 channel realizations of a 3×3 FD channel, testing the probability that the synchronous IWFA converges in X steps, which are then plotted in Fig. 5b.

The probability that the asynchronous IWFA converges to a Nash equilibrium in X steps increases as γ increases. It implies that the average number of iterations, which is required by IWFA to reach a Nash equilibrium, reduces with an increase of γ . Therefore, the computational efficiency of IWFA is improved if the gain of the direct channel over the self-interference channel increases.

In Fig. 6, we compare the performance of FD Nash equilibrium with half-duplex TDMA in terms of the achievable sum-rate. Each node is equipped with $M = 3$ transmit antennas and

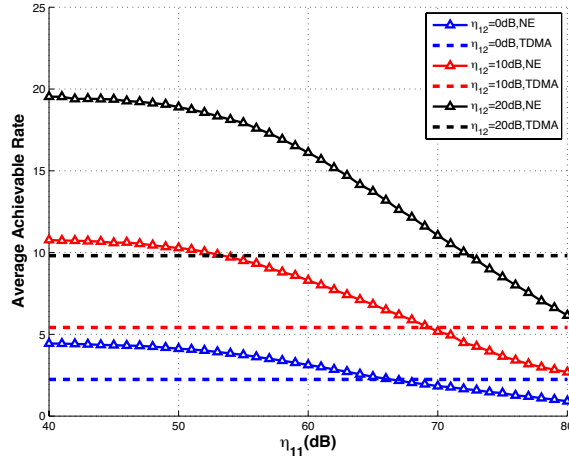


Fig. 6: Average achievable sum-rate for a symmetric MIMO two-way FD channel with $\beta = -60$ dB, $P_1 = P_2 = 10$ and $M = N = 3$.

$N = 3$ receive antennas with the transmit power constraints $P_1 = P_2 = 1$. The transmit front-end noise level is fixed with $\beta = -60$ dB. For simplicity, the FD channel is assumed to be symmetric i.e., $\mathbf{H}_{12} = \mathbf{H}_{21}$ and $\mathbf{H}_{11} = \mathbf{H}_{22}$ with $\eta_{11} = \eta_{22}$ and $\eta_{12} = \eta_{21}$, where $\mathbf{H}_{ij} \sim \mathcal{CN}(\mathbf{0}, \mathbf{I}_{MN})$. The curves are averaged over 1000 independent channel realizations.

The performances of both FD NE and half-duplex TDMA are improved as the direct channel gain η_{ij} increases. If the self-interference channel gain η_{ii} is less than 50dB, then the direct channel gain η_{ij} dominates the performance of the FD channel in terms of the achievable rate. The achievable sum-rate of FD NE is close to double that of half-duplex TDMA, implying that it is nearly optimal to operate at FD NE within the low η_{ii} region. Beyond the low η_{ii} region, the sum-rate of FD NE linearly decreases with the increase of η_{ii} . This is due to the fact that the residual self-interference leads the performance of the FD channel beyond the low η_{ii} region. In contrast, TDMA works in half-duplex mode, thus the performance of TDMA is not affected by the self-interference. It follows that the gap between FD NE and half-duplex TDMA decreases as η_{ii} increases with a given η_{ij} . Interestingly, NE and TDMA perform evenly at $\eta_{ii} = 67$ dB, $\eta_{ii} = 69$ dB and $\eta_{ii} = 72$ dB, if $\eta_{ij} = 0$ dB, $\eta_{ij} = 10$ dB and $\eta_{ij} = 20$ dB respectively. It implies that the tradeoff between FD NE and half-duplex TDMA is mainly determined by the self-interference channel gain η_{ii} instead of the direct channel gain η_{ij} . Moreover, the achievable sum-rate of NE is smaller than that of TDMA with regardless of the value of η_{ij} if η_{ii} is beyond

72dB. It follows that the NE of the FD two-way channel can bring extra benefits than the half-duplex TDMA two-way channel only if the self-interference channel gain can be suppressed to be lower than 72dB.

VII. CONCLUSION

We considered the MIMO point-to-point full-duplex wireless network under the imperfect transmit front-end chains. The network was modeled by a MIMO two-way full-duplex channel with transmit front-end noise, which was then studied from a game-theoretic view. We characterized the Pareto boundary for a MISO two-way full-duplex channel in presence of the transmit front-end noise. Using the decoupling technique and SDP reformulation, we proposed a method to obtain the entire Pareto boundary by solving a family of convex SDP problems, rather than the original non-convex problems. We showed that any rate pair on the Pareto boundary can be achieved by the beamforming transmission strategy. Moreover, we provided the closed-form solution for the optimal beamforming weights of the MISO full-duplex two-way channel.

For the general MIMO full-duplex two-way channel, we achieved the competitive optimality by establishing the existence and the uniqueness of Nash equilibrium. We then modified the classical iterative waterfilling algorithm to efficiently reach the NE for a MIMO two-way full-duplex channel. Through our numerical results, we demonstrated that the transmit front-end noise level β and the direct-to-self-interference channel gain ratio γ can influence the full-duplex NE from the following perspectives. First, the computational efficiency of reaching a full-duplex NE improves with the reduction of β or the increase of γ . Second, the stability of operating on full-duplex NE improves as β decreases or γ increases. Finally, we found that the self-interference channel gain $\eta_{ii} = 72\text{dB}$ is the threshold, beyond which the full-duplex NE is outperformed by the half-duplex TDMA in achievable rates.

VIII. APPENDIX

A. Proof of Theorem 1

We prove Theorem 1 by the primal-dual method. Note that problem (13) is feasible and bounded. It follows that its dual problem is also feasible and bounded [13]. Assume Q^* is an

optimal solution for problem (13). From [13], problem (13) has the dual problem as follows:

$$\min_{\lambda_1, \lambda_2} \lambda_1 z_i + \lambda_2 P \quad (38)$$

$$\text{subject to } \mathbf{Z} = \mathbf{C}_i - \lambda_1 \mathbf{A}_i - \lambda_2 \mathbf{I} \succeq 0.$$

where $P = \text{tr}(\mathbf{Q}^*)$. Assume $((\lambda_1^*, \lambda_2^*), \mathbf{Z}^*)$ are the optimal solutions for (38). We denote the rank of \mathbf{Q}^* by r . We assume $r > 1$. Following that \mathbf{Q}^* is positive semi-definite, \mathbf{Q}^* can then be written as $\mathbf{Q}^* = \mathbf{V}\mathbf{V}^\dagger$ via the singular-value decomposition where $\mathbf{V} \in \mathbb{C}^{M \times r}$.

Next, we consider the following two linear equations defined by \mathbf{A}_i and \mathbf{V} :

$$\begin{cases} \text{tr}(\mathbf{V}^\dagger \mathbf{A}_i \mathbf{V} \mathbf{X}) = 0 \\ \text{tr}(\mathbf{X}) = 0 \end{cases} \quad (39)$$

where the unknown matrix $\mathbf{X} \in \mathbb{H}^r$ contains r^2 real-valued unknowns, that is, $\frac{r(r+1)}{2}$ for the real part and $\frac{r(r-1)}{2}$ for the imaginary part.

The linear system (39) must have a non-zero solution, denoted by \mathbf{X}^* , since it has r^2 unknowns where $r \geq 2$. By decomposing the Hermitian matrix \mathbf{X}^* , we obtain $\mathbf{X}^* = \mathbf{U}\mathbf{\Sigma}\mathbf{U}^\dagger$, where \mathbf{U} is an r dimensional unitary matrix and $\mathbf{\Sigma}$ is the diagonal matrix, $\mathbf{\Sigma} = \text{Diag}(\sigma_1, \dots, \sigma_r)$. Without loss of generality, we assume $|\sigma_1| \geq |\sigma_2| \cdots \geq |\sigma_r|$. Non-zero matrix \mathbf{X}^* has at least one non-trivial eigenvalue, thus $|\sigma_1| > 0$. Next, we construct a new matrix as follows:

$$\mathbf{Q}_{(1)}^* = \mathbf{V}(\mathbf{I} - \frac{1}{\sigma_1} \mathbf{X}^*)\mathbf{V}^\dagger. \quad (40)$$

Note that $\mathbf{I} - \frac{1}{\sigma_1} \mathbf{X}^* \succeq 0$. It follows that $\mathbf{Q}_{(1)}^*$ is semi-positive definite. Next, we show that $\mathbf{Q}_{(1)}^*$ is also an optimal solution for problem (13). Note that $\mathbf{Q}_{(1)}^*$ is optimal for problem (13) if and only if $(\mathbf{Q}_{(1)}^*, (\lambda_1^*, \lambda_2^*), \mathbf{Z}^*)$ satisfies the KKT conditions, including the primal feasibility, the dual feasibility and the complementarity [24]. As $((\lambda_1^*, \lambda_2^*), \mathbf{Z}^*)$ is unchanged, the dual feasibility is automatically satisfied. Therefore, we need only to prove the primal feasibility and the complementarity of $\mathbf{Q}_{(1)}^*$.

$\mathbf{Q}_{(1)}^*$ is a feasible solution for problem (13), since the following two equations hold for $\mathbf{Q}_{(1)}^*$,

$$\begin{aligned} \text{tr}(\mathbf{A}_i \mathbf{Q}_{(1)}^*) &= \text{tr}(\mathbf{A}_i \mathbf{V}(\mathbf{I} - \frac{1}{\sigma_1} \mathbf{X}^*)\mathbf{V}^\dagger) \\ &= \text{tr}(\mathbf{V}^\dagger \mathbf{A}_i \mathbf{V} \mathbf{I}) - \frac{1}{\sigma_1} \text{tr}(\mathbf{V}^\dagger \mathbf{A}_i \mathbf{V} \mathbf{X}^*) = z_i, \end{aligned} \quad (41)$$

$$\begin{aligned} \text{tr}(\mathbf{Q}_{(1)}^*) &= \text{tr}(\mathbf{V}(\mathbf{I} - \frac{1}{\sigma_1} \mathbf{X}^*)\mathbf{V}^\dagger) \\ &= \text{tr}(\mathbf{V}^\dagger \mathbf{V} \mathbf{I}) - \frac{1}{\sigma_1} \text{tr}(\mathbf{V}^\dagger \mathbf{V} \mathbf{X}^*) = P. \end{aligned} \quad (42)$$

To show the complementarity, note that $\mathbf{tr}(\mathbf{Q}^* \mathbf{Z}^*) = \mathbf{tr}(\mathbf{V}^\dagger \mathbf{Z}^* \mathbf{V}) = 0$ and $\mathbf{V}^\dagger \mathbf{Z}^* \mathbf{V} \succeq 0$ implies that $\mathbf{V}^\dagger \mathbf{Z}^* \mathbf{V} = 0$. It follows that

$$\begin{aligned} \mathbf{tr}(\mathbf{Q}_{(1)}^* \mathbf{Z}^*) &= \mathbf{tr}(\mathbf{V}(\mathbf{I} - \frac{1}{\sigma_1} \mathbf{X}^*) \mathbf{V}^\dagger \mathbf{Z}^*) \\ &= \mathbf{tr}((\mathbf{I} - \frac{1}{\sigma_1} \mathbf{X}^*) \mathbf{V}^\dagger \mathbf{Z}^* \mathbf{V}) = 0. \end{aligned} \quad (43)$$

Therefore, $\mathbf{Q}_{(1)}^*$ is an optimal solution for problem (13). Furthermore, the rank of $\mathbf{Q}_{(1)}^*$ is strictly smaller than r since $\text{rank}(\mathbf{Q}_{(1)}^*) = \text{rank}(\mathbf{I} - \frac{1}{\sigma_1} \mathbf{X}^*) < r$.

We can repeat this process as $\mathbf{Q}^*, \mathbf{Q}_{(1)}^*, \mathbf{Q}_{(2)}^*, \dots$, until $\text{rank}(\mathbf{Q}_{(k)}^*) \leq \sqrt{2}$. In other words, the rank of the optimal solution can be strictly decreasing to $\text{rank}(\mathbf{Q}_{(k)}^*) \leq \sqrt{2}$, that is, $\text{rank}(\mathbf{Q}_{(k)}^*) = 1$.

B. Properties of The Best-Response Function $\mathcal{B}(\cdot)$

Introducing the constant P_i and the matrices $\{\mathbf{H}_{ij}\}_{i,j \in \{1,2\}}$, the best-response function $\mathcal{B}_i(\mathbf{Q}_j)$ denotes the optimal solution of the following optimization problem:

$$\begin{aligned} \max_{\mathbf{Q}_i} \quad & \log \det(\mathbf{I} + \eta_{ij} \mathbf{H}_{ij}^\dagger \Sigma_j^{-1} \mathbf{H}_{ij} \mathbf{Q}_i) \\ \text{subject to} \quad & \mathbf{Q}_i \in \mathcal{X}_i, \end{aligned} \quad (44)$$

where $i, j \in \{1, 2\}$ and $i \neq j$; $\Sigma_i \triangleq \mathbf{I} + \beta \eta_{ii} \mathbf{H}_{ii} \text{diag}(\mathbf{Q}_i) \mathbf{H}_{ii}^\dagger$ which is a full-rank square matrix.

According to [11, Lemma 11.1 and Lemma 11.2], problem (44) can be equivalent to

$$\begin{aligned} \min_{\mathbf{Q}_i} \quad & \|\mathbf{Q}_i - \mathbf{X}_0(\mathbf{Q}_j)\|_F \\ \text{subject to} \quad & \mathbf{Q}_i \in \mathcal{X}_i, \end{aligned} \quad (45)$$

where \mathcal{X}_i is a non-empty closed convex set; $\mathbf{X}_0(\mathbf{Q}_j) = -\left(\eta_{ij} \mathbf{H}_{ij}^\dagger \Sigma_j^{-1} \mathbf{H}_{ij}\right)^{-1} - c_i \mathbf{P}_{\mathcal{N}(\mathbf{H}_{ij})}$ with the positive constant c_i that can be chosen independent of \mathbf{Q}_j and the matrix $\mathbf{P}_{\mathcal{N}(\mathbf{H}_{ij})}$ that depends only on the channel matrix \mathbf{H}_{ji} . It follows that $\mathcal{B}_i(\mathbf{Q}_j)$ represents the point in \mathcal{X}_i which is closest to $\mathbf{X}_0(\mathbf{Q}_j)$. The best-response function $\mathcal{B}(\cdot)$ can then be alternatively interpreted as a metric projection which projects the matrix $\mathbf{X}_0(\mathbf{Q}_j)$ onto the set \mathcal{X}_i .

The interpretation of the function $\mathcal{B}(\cdot)$ as the metric projection implies the non-expansive property as follows:

$$\|\mathcal{B}_i(\mathbf{Q}_j^{(1)}) - \mathcal{B}_i(\mathbf{Q}_j^{(2)})\|_F \leq \|\mathbf{X}_0(\mathbf{Q}_j^{(1)}) - \mathbf{X}_0(\mathbf{Q}_j^{(2)})\|_F, \quad \forall \mathbf{Q}_j^{(1)}, \mathbf{Q}_j^{(2)} \in \mathbb{C}^{M \times M}. \quad (46)$$

Building on the continuity of the metric projection and using the continuity of $\mathbf{X}_0(\mathbf{Q}_i)$ on \mathbf{Q}_i , one can obtain the continuous property of the best-response function $\mathcal{B}(\mathbf{Q}_i)$ on \mathbf{Q}_i .

C. Proof of Lemma 3

Following (20), a Nash equilibrium is equivalent to a fixed-point of the mapping Φ in (19). Thus, we will use the following results in the fixed-point theory from [11, 25] to show the existence of NE.

Proposition 1. Given a mapping $\mathcal{T} : \mathcal{X} \mapsto \mathcal{X}$. If \mathcal{X} is nonempty, convex and compact subset of a finite-dimensional normed vector space and \mathcal{T} is a continuous mapping, then \mathcal{T} has at least one fixed-point.

Using Proposition 1, it suffices to show the existence of fixed-points for the water-filling mapping Φ in (19). The water-filling mapping Φ in (19) is defined on the set $\mathcal{X}_1 \times \mathcal{X}_2$, where $\mathcal{X}_i = \{\mathbf{Q} \in \mathbb{H}^M \mid \mathbf{Q} \succeq 0, \text{tr}(\mathbf{Q}) \leq P_i\}$. It follows from the results in [13] that \mathcal{X}_i is a convex and compact subset of \mathbb{C}^{M^2} for any $P_i \in \mathbb{R}$. Thus, \mathcal{X} is nonempty, convex and compact set with a finite dimension for any transmit power constraints P_1 and P_2 . In Appendix B, We prove the continuity of the Best-response function $\mathcal{B}_i(\cdot)$ on \mathcal{X}_i for any given set of channel matrices $\{\mathbf{H}_{ij}\}_{i,j \in \{1,2\}}$. It follows that the mapping Φ is continuous on $\mathcal{X}_1 \times \mathcal{X}_2$ for any channel realization. Lemma 3 is then an immediate result following from Proposition 1.

D. Proof of Lemma 4

Following the equivalence built in (20), we can instead derive sufficient conditions for the uniqueness of fixed-point in mapping Φ . To do so, we need to use the following Proposition from [25].

Proposition 2 (Uniqueness of fixed-point). Let $\mathcal{T} : \mathcal{X} \mapsto \mathcal{X}$ be a mapping defined on a finite-dimensional set \mathcal{X} . If \mathcal{T} is a contraction with respect to some norm $\|\cdot\|$, that is, there exists some scalar $\alpha \in [0, 1)$ such that

$$\|\mathcal{T}(x^{(1)}) - \mathcal{T}(x^{(2)})\| \leq \alpha \|x^{(1)} - x^{(2)}\|, \forall x^{(1)}, x^{(2)} \in \mathcal{X}. \quad (47)$$

Then, there exists at most one fixed point of \mathcal{T} .

To apply Proposition 2 for the mapping Φ in (19), we need to define a suitable norm on the vector space $\mathbb{H}^M \times \mathbb{H}^M$ in which the mapping Φ is defined. Inspired by the work in [9], we introduce the weighted-maximum norm, which is defined as:

$$\|(\mathbf{X}_1, \mathbf{X}_2)\|_F^{\mathbf{w}} \triangleq \max_{i \in \{1,2\}} \frac{\|\mathbf{X}_i\|_F}{w_i}, \quad (48)$$

where $\mathbf{X}_i \in \mathbb{H}^M$, $\|\cdot\|_F$ is the Frobenius norm and $\mathbf{w} = [w_1, w_2] > 0$ is any positive vector.

Next, we focus on the contraction property of the mapping Φ with respect to the weighted-maximum norm $\|\cdot\|_F^{\mathbf{w}}$. That is to show the conditions for the existence of $\alpha \in [0, 1)$, $\mathbf{w} > 0$ such that

$$\begin{aligned} \left\| \Phi \left(\mathbf{Q}_1^{(1)}, \mathbf{Q}_2^{(1)} \right) - \Phi \left(\mathbf{Q}_1^{(2)}, \mathbf{Q}_2^{(2)} \right) \right\|_F^{\mathbf{w}} &\leq \alpha \left\| \left(\mathbf{Q}_1^{(1)}, \mathbf{Q}_2^{(1)} \right) - \left(\mathbf{Q}_1^{(2)}, \mathbf{Q}_2^{(2)} \right) \right\|_F^{\mathbf{w}}, \quad (49) \\ \forall \left(\mathbf{Q}_1, \mathbf{Q}_2 \right) &\in \mathcal{X}_1 \times \mathcal{X}_2. \end{aligned}$$

For the convenience of the notation, we introduce e_i and e_{Φ_i} defined as

$$e_i = \left\| \mathbf{Q}_i^{(1)} - \mathbf{Q}_i^{(2)} \right\|_F, \quad e_{\Phi_i} \triangleq \left\| \mathcal{B}_i \left(\mathbf{Q}_j^{(1)} \right) - \mathcal{B}_i \left(\mathbf{Q}_j^{(2)} \right) \right\|_F, \quad (50)$$

where $i, j \in \{1, 2\}$ and $i \neq j$.

Given two sets of strategies $\left(\mathbf{Q}_1^{(1)}, \mathbf{Q}_2^{(1)} \right), \left(\mathbf{Q}_1^{(2)}, \mathbf{Q}_2^{(2)} \right) \in \mathcal{X}_1 \times \mathcal{X}_2$, we can rewrite the left and right side of (49) in terms of the vector $\mathbf{e} = [e_1, e_2]^T$ and $\mathbf{e}_{\Phi} = [e_{\Phi_1}, e_{\Phi_2}]^T$ as

$$\|\mathbf{e}\|_{\infty}^{\mathbf{w}} = \left\| \left(\mathbf{Q}_1^{(1)}, \mathbf{Q}_2^{(1)} \right) - \left(\mathbf{Q}_1^{(2)}, \mathbf{Q}_2^{(2)} \right) \right\|_F^{\mathbf{w}}, \quad (51)$$

$$\|\mathbf{e}_{\Phi}\|_{\infty}^{\mathbf{w}} = \left\| \Phi \left(\mathbf{Q}_1^{(1)}, \mathbf{Q}_2^{(1)} \right) - \Phi \left(\mathbf{Q}_1^{(2)}, \mathbf{Q}_2^{(2)} \right) \right\|_F^{\mathbf{w}}, \quad (52)$$

where the norm $\|\mathbf{x}\|_{\infty}^{\mathbf{w}}$ of a vector $\mathbf{x} \in \mathbb{C}^{K \times 1}$ is defined as $\|\mathbf{x}\|_{\infty}^{\mathbf{w}} \triangleq \max_{i \in \{1 \dots K\}} \frac{\|x_i\|_F}{w_i}$ with some $\mathbf{w} > 0$.

The inequality in (49) can then be rewritten as

$$\|\mathbf{e}_{\Phi}\|_{\infty}^{\mathbf{w}} \leq \alpha \|\mathbf{e}\|_{\infty}^{\mathbf{w}}. \quad (53)$$

We start to assume that the direct channels \mathbf{H}_{ij} are full row-rank. We continue to show the

expression of α by using the similar procedure in [9]. First, we have

$$\begin{aligned} e_{\Phi_i} &= \left\| \mathcal{B}_i(\mathbf{Q}_j^{(1)}) - \mathcal{B}_i(\mathbf{Q}_j^{(2)}) \right\|_F \\ &\leq \left\| \mathbf{X}_0(\mathbf{Q}_j^{(1)}) - \mathbf{X}_0(\mathbf{Q}_j^{(2)}) \right\|_F \end{aligned} \quad (54)$$

$$= \left\| \left(\left(\eta_{ij} \mathbf{H}_{ij}^\dagger \Sigma_j^{(1)-1} \mathbf{H}_{ij} \right)^{-1} + c_j \mathbf{P}_{\mathcal{N}(\mathbf{H}_{ij})} \right) - \left(\left(\eta_{ij} \mathbf{H}_{ij}^\dagger \Sigma_j^{(2)-1} \mathbf{H}_{ij} \right)^{-1} + c_j \mathbf{P}_{\mathcal{N}(\mathbf{H}_{ij})} \right) \right\|_F \quad (55)$$

$$= \left\| \frac{\beta}{\gamma_j} \mathbf{H}_{ij}^{-1} \mathbf{H}_{jj} \left(\text{diag}(\mathbf{Q}_j^{(1)}) - \text{diag}(\mathbf{Q}_j^{(2)}) \right) \mathbf{H}_{jj}^\dagger \mathbf{H}_{ij}^{-\dagger} \right\|_F \quad (56)$$

$$\leq \rho \left(\frac{\beta}{\gamma_j} \mathbf{H}_{jj}^\dagger \mathbf{H}_{ij}^{-\dagger} \mathbf{H}_{ij}^{-1} \mathbf{H}_{jj} \right) \cdot \left\| \text{diag}(\mathbf{Q}_j^{(1)}) - \text{diag}(\mathbf{Q}_j^{(2)}) \right\|_F \quad (57)$$

$$\leq \rho \left(\frac{\beta}{\gamma_j} \mathbf{H}_{jj}^\dagger \mathbf{H}_{ij}^{-\dagger} \mathbf{H}_{ij}^{-1} \mathbf{H}_{jj} \right) \cdot \left\| \mathbf{Q}_j^{(1)} - \mathbf{Q}_j^{(2)} \right\|_F$$

$$= \rho \left(\frac{\beta}{\gamma_j} \mathbf{H}_{jj}^\dagger \mathbf{H}_{ij}^{-\dagger} \mathbf{H}_{ij}^{-1} \mathbf{H}_{jj} \right) e_j$$

where (54) follows from inequality (46); (55) follows from (45); (56) follows from the reverse-order law for the generalized inverse i.e., $(\mathbf{A}^\dagger \mathbf{X} \mathbf{A})^{-1} = \mathbf{A}^{-1} \mathbf{X}^{-1} \mathbf{A}^{-\dagger}$ [11], which is valid if \mathbf{A} is full row-rank matrix; (57) follows from the triangle inequality $\|\mathbf{A} \mathbf{X} \mathbf{A}^\dagger\|_F \leq \rho(\mathbf{A}^\dagger \mathbf{A}) \|\mathbf{X}\|_F$.

Define the matrix \mathbf{S} as follows:

$$[\mathbf{S}]_{ij} = \begin{cases} \rho \left(\frac{\beta}{\gamma_j} \mathbf{H}_{jj}^\dagger \mathbf{H}_{ij}^{-\dagger} \mathbf{H}_{ij}^{-1} \mathbf{H}_{jj} \right), & \text{if } i \neq j, \\ 0, & \text{otherwise.} \end{cases} \quad (58)$$

We then have

$$\|e_{\Phi}\|_\infty^w \leq \|\mathbf{S}e\|_\infty^w \leq \|\mathbf{S}\|_\infty^w \cdot \|e\|_\infty^w. \quad (59)$$

By setting $\alpha = \|\mathbf{S}\|_\infty^w$, Φ in (19) is a contraction with respect to the weighted-maximum norm if there exists some $w > 0$ such that $\|\mathbf{S}\|_\infty^w < 1$. Note that all entries of \mathbf{S} are non-negative. According to [23], $\|\mathbf{S}\|_\infty^w < 1$ for some $w > 0$ if and only if $\rho(\mathbf{S}) < 1$. Finally, the radius of \mathbf{S} can be easily obtained

$$\rho(\mathbf{S}) = \sqrt{\rho \left(\frac{\beta}{\gamma_1} \mathbf{H}_{11}^\dagger \mathbf{H}_{21}^{-\dagger} \mathbf{H}_{21}^{-1} \mathbf{H}_{11} \right) \rho \left(\frac{\beta}{\gamma_2} \mathbf{H}_{22}^\dagger \mathbf{H}_{12}^{-\dagger} \mathbf{H}_{12}^{-1} \mathbf{H}_{22} \right)}, \quad (60)$$

which leads to the condition (21).

E. Proof of Theorem 2

The main challenge in extending Lemma 4 to the general full-duplex channel is that the reverse-order law for the generalized inverse, which is used in (56), is valid only under the full row-rank assumption of \mathbf{H}_{ij} . In general, one can only have the inequality $(\mathbf{A}^\dagger \mathbf{X} \mathbf{A})^{-1} \preceq \mathbf{A}^{-1} \mathbf{X}^{-1} \mathbf{A}^{-\dagger}$. For the sake of simplicity, we first focus on the strictly full-rank case, where the direct channel matrices $\{\mathbf{H}_{ij}\}_{i,j \in \{1,2\}, i \neq j}$ are with full column-rank. Using the notations and following the procedure in the proof of Lemma 4, we obtain

$$\begin{aligned}
e_{\Phi_i} &= \left\| \mathcal{B}_i(\mathbf{Q}_j^{(1)}) - \mathcal{B}_i(\mathbf{Q}_j^{(2)}) \right\|_F \\
&\leq \left\| \mathbf{X}_0(\mathbf{Q}_j^{(1)}) - \mathbf{X}_0(\mathbf{Q}_j^{(2)}) \right\|_F \\
&= \left\| \left(\left(\eta_{ij} \mathbf{H}_{ij}^\dagger \Sigma_j^{(1)-1} \mathbf{H}_{ij} \right)^{-1} + c_j \mathbf{P}_{\mathcal{N}(\mathbf{H}_{ij})} \right) - \left(\left(\eta_{ij} \mathbf{H}_{ij}^\dagger \Sigma_j^{(2)-1} \mathbf{H}_{ij} \right)^{-1} + c_j \mathbf{P}_{\mathcal{N}(\mathbf{H}_{ij})} \right) \right\|_F \\
&= \left\| \left(\eta_{ij} \mathbf{H}_{ij}^\dagger \Sigma_j^{(1)-1} \mathbf{H}_{ij} \right)^{-1} - \left(\eta_{ij} \mathbf{H}_{ij}^\dagger \Sigma_j^{(2)-1} \mathbf{H}_{ij} \right)^{-1} \right\|_F
\end{aligned} \tag{61}$$

The strictly full column-rank of \mathbf{H}_{ij} implies that \mathbf{H}_{ij} is deficient in row-rank, thus we cannot derive the upper-bound for (61), as was done in (56). Thus, we need to develop an approach suitable for deriving the upper-bound in the full column-rank case. To this end, we introduce the function $\mathbf{P}_i(\mathbf{X}) : \mathcal{Q}_i \mapsto \mathbb{C}^{M \times M}$ as follows,

$$\mathbf{P}_i(\mathbf{X}) = \left(\mathbf{H}_{ij}^\dagger \left(\mathbf{I} + \beta \eta_{jj} \mathbf{H}_{jj} \mathbf{X} \mathbf{H}_{jj}^\dagger \right)^{-1} \mathbf{H}_{ij} \right)^{-1}, \tag{62}$$

where $\mathcal{Q}_i \triangleq \{\mathbf{Q} \in \mathbb{H}_+^M \mid \mathbf{tr}(\mathbf{Q}) = P_i\}$ is a convex set. Since \mathbf{H}_{ij} is with the full column-rank that $\mathbf{P}_i(\mathbf{X})$ is invertible, which implies that $\mathbf{P}_i(\mathbf{X})$ is continuous on \mathcal{Q}_i and differentiable on the interior of \mathcal{Q}_i [26]. Invoking the mean-value theorem in [11], we obtain that for any given $\mathbf{X}, \mathbf{Y} \in \mathcal{Q}_i$ there exists $\boldsymbol{\xi} = \alpha \mathbf{X} + \beta \mathbf{Y}$ with some $\alpha, \beta \geq 0$ and $\alpha + \beta = 1$ such that

$$\|\mathbf{P}_i(\mathbf{Y}) - \mathbf{P}_i(\mathbf{X})\|_F \leq \|\mathbf{D}_{\mathbf{X}} \mathbf{P}_i(\boldsymbol{\xi})\|_2 \|\mathbf{Y} - \mathbf{X}\|_F, \tag{63}$$

where $\mathbf{D}_{\mathbf{X}} \mathbf{P}_i$ denotes the derivative of the function $\mathbf{P}_i(\mathbf{X})$ with respect to \mathbf{X} , defined by the following equation [27]:

$$\text{dvec}(\mathbf{P}_i) = (\mathbf{D}_{\mathbf{X}} \mathbf{P}_i) \text{dvec}(\mathbf{X}) + (\mathbf{D}_{\mathbf{X}^\dagger} \mathbf{P}_i) \text{dvec}(\mathbf{X}^\dagger). \tag{64}$$

The above identity implies that we can derive $\mathbf{D}_{\mathbf{X}} \mathbf{P}_i$ by differentiating and vectorizing $\mathbf{P}_i(\mathbf{X})$. For the convenience of notation, we denote $\mathbf{R}_j(\mathbf{X}) = \mathbf{I} + \beta \eta_{jj} \mathbf{H}_{jj} \mathbf{X} \mathbf{H}_{jj}^\dagger$, simplified as \mathbf{R}_j .

Then,

$$\begin{aligned}
\text{dvec}(\mathbf{P}_i) &= \text{vec}(\text{d}\mathbf{P}_i) = -\text{vec}(\mathbf{P}_i(\text{d}\mathbf{P}_i^{-1})\mathbf{P}_i) \\
&= \text{vec}\left(\mathbf{P}_i \cdot \text{d}\left(\mathbf{H}_{ij}^\dagger \mathbf{R}_j^{-1} \mathbf{H}_{ij}\right) \cdot \mathbf{P}_i\right) \\
&= \beta \eta_{jj} \text{vec}\left(\mathbf{P}_i \mathbf{H}_{ij}^\dagger \mathbf{R}_j^{-1} \mathbf{H}_{jj} \cdot \text{d}(\mathbf{X}) \cdot \mathbf{H}_{jj}^\dagger \mathbf{R}_j^{-1} \mathbf{H}_{ij} \mathbf{P}_i\right) \\
&= \beta \eta_{jj} \text{vec}\left(\mathbf{G}_i(\mathbf{X}) \text{d}(\mathbf{X}) \overline{\mathbf{G}_i(\mathbf{X})}\right) \\
&= \beta \eta_{jj} \left(\overline{\mathbf{G}_i(\mathbf{X})} \otimes \mathbf{G}_i(\mathbf{X})\right) \text{dvec}(\mathbf{X}),
\end{aligned} \tag{65}$$

where $\mathbf{G}_i(\mathbf{X}) = \mathbf{P}_i \mathbf{H}_{ij}^\dagger \mathbf{R}_j^{-1} \mathbf{H}_{jj}$ is a Hermitian matrix; \otimes denotes the Kronecker product; (65) follows from the invertibility of $\mathbf{P}_i(\mathbf{X})$; (66) follows from the result in [28]. (64) and (66) indicate that $\mathbf{D}_\mathbf{X} \mathbf{P}_i = \beta \left(\overline{\mathbf{G}_i(\mathbf{X})} \otimes \mathbf{G}_i(\mathbf{X})\right)$. Invoking (63), we obtain

$$\|\mathbf{P}_i(\mathbf{Y}) - \mathbf{P}_i(\mathbf{X})\|_F \leq \beta \eta_{jj} \|\overline{\mathbf{G}_i(\boldsymbol{\xi})} \otimes \mathbf{G}_i(\boldsymbol{\xi})\|_2 \|\mathbf{Y} - \mathbf{X}\|_F. \tag{67}$$

We can further investigate (66) by

$$\begin{aligned}
\|\overline{\mathbf{G}_i(\boldsymbol{\xi})} \otimes \mathbf{G}_i(\boldsymbol{\xi})\|_2 &= \sqrt{\rho\left(\left(\overline{\mathbf{G}_i(\boldsymbol{\xi})} \otimes \mathbf{G}_i(\boldsymbol{\xi})\right)^\dagger \left(\overline{\mathbf{G}_i(\boldsymbol{\xi})} \otimes \mathbf{G}_i(\boldsymbol{\xi})\right)\right)} \\
&= \sqrt{\rho\left(\left(\mathbf{G}_i(\boldsymbol{\xi})^T \otimes \mathbf{G}_i^\dagger(\boldsymbol{\xi})\right) \left(\overline{\mathbf{G}_i(\boldsymbol{\xi})} \otimes \mathbf{G}_i(\boldsymbol{\xi})\right)\right)} \\
&= \sqrt{\rho\left(\left(\mathbf{G}_i^T(\boldsymbol{\xi}) \overline{\mathbf{G}_i(\boldsymbol{\xi})}\right) \otimes \left(\mathbf{G}_i^\dagger(\boldsymbol{\xi}) \mathbf{G}_i(\boldsymbol{\xi})\right)\right)} \\
&= \rho\left(\mathbf{G}_i^\dagger(\boldsymbol{\xi}) \mathbf{G}_i(\boldsymbol{\xi})\right).
\end{aligned} \tag{68}$$

Each step in (68) follows from the property of the Kronecker product. Note that the orthogonal projection onto the range of $\mathbf{R}_j^{-1/2} \mathbf{H}_{ij}^\dagger$ i.e., $\text{Ran}(\mathbf{R}_j^{-1/2} \mathbf{H}_{ij}^\dagger)$, is defined as

$$\mathbf{P}_{\mathbf{R}_j} = \mathbf{R}_j^{-1/2} \mathbf{H}_{ij} \mathbf{P}_i \mathbf{H}_{ij}^\dagger \mathbf{R}_j^{-1/2}. \tag{69}$$

Then, $\mathbf{G}_i(\boldsymbol{\xi})$ can be rewritten in terms of $\mathbf{P}_{\mathbf{R}_j}$ as $\mathbf{G}_i(\boldsymbol{\xi}) = \mathbf{H}_{ij}^{-1} \mathbf{R}_j^{1/2} \mathbf{P}_{\mathbf{R}_j} \mathbf{R}_j^{-1/2} \mathbf{H}_{jj}$. It follows that

$$\begin{aligned}
\rho\left(\mathbf{G}_i^\dagger(\boldsymbol{\xi}) \mathbf{G}_i(\boldsymbol{\xi})\right) &= \rho\left(\mathbf{H}_{jj}^\dagger \mathbf{R}_j^{-1/2} \mathbf{P}_{\mathbf{R}_j}^\dagger \mathbf{R}_j^{1/2} \mathbf{H}_{ij}^{-\dagger} \mathbf{H}_{ij}^{-1} \mathbf{R}_j^{1/2} \mathbf{P}_{\mathbf{R}_j} \mathbf{R}_j^{-1/2} \mathbf{H}_{jj}\right) \\
&\leq \rho\left(\mathbf{H}_{jj}^\dagger \mathbf{H}_{jj}\right) \rho\left(\mathbf{R}_j^{-1}(\boldsymbol{\xi})\right) \rho\left(\mathbf{H}_{ij}^{-\dagger} \mathbf{H}_{ij}^{-1}\right) \rho\left(\mathbf{R}_j(\boldsymbol{\xi})\right).
\end{aligned} \tag{70}$$

Let $\mathbf{X} = \text{diag}(\mathbf{Q}_j^{(1)})$, $\mathbf{Y} = \text{diag}(\mathbf{Q}_j^{(2)})$. We can continue estimate (61),

$$\begin{aligned} e_{\Phi_i} &\leq \left\| \left(\eta_{ij} \mathbf{H}_{ij}^\dagger \Sigma_j^{(1)-1} \mathbf{H}_{ij} \right)^{-1} - \left(\eta_{ij} \mathbf{H}_{ij}^\dagger \Sigma_j^{(2)-1} \mathbf{H}_{ij} \right)^{-1} \right\|_F \\ &= \frac{1}{\eta_{ij}} \|\mathbf{P}_i(\mathbf{Y}) - \mathbf{P}_i(\mathbf{X})\|_F \end{aligned} \quad (71)$$

$$\leq \frac{\beta \eta_{jj}}{\eta_{ij}} \rho \left(\mathbf{H}_{jj}^\dagger \mathbf{H}_{jj} \right) \rho \left(\mathbf{H}_{ij}^{-\dagger} \mathbf{H}_{ij}^{-1} \right) \rho \left(\mathbf{R}_j^{-1}(\boldsymbol{\xi}) \right) \rho \left(\mathbf{R}_j(\boldsymbol{\xi}) \right) \|\mathbf{Y} - \mathbf{X}\|_F \quad (72)$$

$$\leq \frac{\beta \eta_{jj}}{\eta_{ij}} \left(1 + \beta \eta_{jj} P_j \rho \left(\mathbf{H}_{jj}^\dagger \mathbf{H}_{jj} \right) \right) \rho \left(\mathbf{H}_{jj}^\dagger \mathbf{H}_{jj} \right) \rho \left(\mathbf{H}_{ij}^{-\dagger} \mathbf{H}_{ij}^{-1} \right) \|\mathbf{Q}_j^{(1)} - \mathbf{Q}_j^{(2)}\|_F \quad (73)$$

$$= \frac{\beta \eta_{jj}}{\eta_{ij}} \left(1 + \beta \eta_{jj} P_j \rho \left(\mathbf{H}_{jj}^\dagger \mathbf{H}_{jj} \right) \right) \rho \left(\mathbf{H}_{jj}^\dagger \mathbf{H}_{jj} \right) \rho \left(\mathbf{H}_{ij}^{-\dagger} \mathbf{H}_{ij}^{-1} \right) e_j. \quad (74)$$

where (71) follows from the definition of $\mathbf{P}_i(\cdot)$ in (62); (72) follows from (67), (68) and (70).

To obtain (73), we use the inequality

$$\mathbf{I} \preceq \mathbf{R}_j(\boldsymbol{\xi}) \preceq \mathbf{I} + \beta \eta_{jj} P_j \mathbf{H}_{jj}^\dagger \mathbf{H}_{jj}. \quad (75)$$

By using (74), we can then derive the sufficient condition of the unique NE for the full column-rank case. The derivation is same as in Lemma 4.

Next, we extend the sufficient condition to the rank deficient case. In order to use the results for the full-rank case, the rank-deficient matrix \mathbf{H}_{ij} should be modified to a lower-dimensional full-rank matrix $\widetilde{\mathbf{H}}_{ij}$, where $\widetilde{\mathbf{H}}_{ij} \in \mathbb{C}^{N \times r}$ with $r = \text{rank}(\mathbf{H}_{ij})$. The singular value decomposition (SVD) writes \mathbf{H}_{ij} as $\mathbf{H}_{ij} = \mathbf{U}_{ij} \Sigma_{ij} \mathbf{V}_{ij}^\dagger$ where \mathbf{U}_{ij} and \mathbf{V}_{ij} are semi-unitary matrices; \mathbf{V}_{ij} is a basis for the row space of \mathbf{H}_{ij} . Define $\widetilde{\mathbf{H}}_{ij} = \mathbf{H}_{ij} \mathbf{V}_{ij}$ and replace \mathbf{H}_{ij} by $\widetilde{\mathbf{H}}_{ij}$. Then, the optimization problem in (9) is modified to the following lower-dimensional optimization problem:

$$\begin{aligned} &\max_{\widetilde{\mathbf{Q}}_i} \log \det(\mathbf{I} + \eta_{ij} \widetilde{\mathbf{H}}_{ij}^\dagger \Sigma_j^{-1} \widetilde{\mathbf{H}}_{ij} \widetilde{\mathbf{Q}}_i) \\ &\text{subject to } \widetilde{\mathbf{Q}}_i \in \widetilde{\mathcal{X}}_i, \end{aligned} \quad (76)$$

where $\widetilde{\mathcal{X}}_i = \left\{ \widetilde{\mathbf{Q}}_i \in \mathbb{H}^r \mid \widetilde{\mathbf{Q}}_i \succeq 0, \text{tr}(\widetilde{\mathbf{Q}}_i) \leq P_i \right\}$ and $\widetilde{\mathbf{H}}_{ij}$ is full column-rank matrix. Denote the optimal solution of problem (76) as $\mathcal{B}_{r_i}(\mathbf{Q}_j)$. Next, by building the equivalence between problem (44) and problem (76) we can show that $\mathcal{B}_i(\mathbf{Q}_j) = \mathbf{V}_{ij} \mathcal{B}_{r_i}(\mathbf{Q}_j) \mathbf{V}_{ij}^\dagger$.

First, for any matrix $\mathbf{Q}_i \in \mathcal{X}_i$, there exists some $\widetilde{\mathbf{Q}}_i \in \widetilde{\mathcal{X}}_i$ such that $\mathbf{Q}_i = \mathbf{V}_{ij} \widetilde{\mathbf{Q}}_i \mathbf{V}_{ij}^\dagger$. Thus, $\mathcal{B}_i(\mathbf{Q}_i) = \mathbf{V}_{ij} \widetilde{\mathbf{Q}}_i^* \mathbf{V}_{ij}^\dagger$, $\widetilde{\mathbf{Q}}_i^* \in \widetilde{\mathcal{X}}_i$. Then, using the identity $\det(\mathbf{I} + \mathbf{A}\mathbf{B}) = \det(\mathbf{I} + \mathbf{B}\mathbf{A})$ we

obtain

$$\begin{aligned}
& \det(\mathbf{I} + \eta_{ij} \mathbf{H}_{ij}^\dagger \Sigma_j^{-1} \mathbf{H}_{ij} \mathcal{B}_i(\mathbf{Q}_j)) \\
&= \det(\mathbf{I} + \eta_{ij} \mathbf{H}_{ij} \mathcal{B}_i(\mathbf{Q}_i) \mathbf{H}_{ij}^\dagger \Sigma_i^{-1}) \\
&= \det(\mathbf{I} + \eta_{ij} \mathbf{H}_{ij} \mathbf{V}_{ij} \widetilde{\mathbf{Q}}_i^* \mathbf{V}_{ij}^\dagger \mathbf{H}_{ij}^\dagger \Sigma_i^{-1}) \\
&= \det(\mathbf{I} + \eta_{ij} \widetilde{\mathbf{H}}_{ij} \widetilde{\mathbf{Q}}_i^* \widetilde{\mathbf{H}}_{ij}^\dagger \Sigma_i^{-1}) \\
&= \det(\mathbf{I} + \eta_{ij} \widetilde{\mathbf{H}}_{ij}^\dagger \Sigma_i^{-1} \widetilde{\mathbf{H}}_{ij} \widetilde{\mathbf{Q}}_i^*).
\end{aligned}$$

$\widetilde{\mathbf{Q}}_i^*$ is a feasible solution of problem (76), implying that the maximum of problem (76) is no smaller than that of problem (44). On the other hand, $\mathbf{V}_{ij} \mathcal{B}_{r_i}(\mathbf{Q}_j) \mathbf{V}_{ij}^\dagger$ is feasible for problem (44). Thus the maximum of problem (76) is no greater than that of problem (44). Therefore, problem (44) and problem (76) are equivalent, implying $\mathcal{B}_i(\mathbf{Q}_j) = \mathbf{V}_{ij} \mathcal{B}_{r_i}(\mathbf{Q}_j) \mathbf{V}_{ij}^\dagger$.

We now can continue to prove Theorem 2. Similar to the proof of the full-rank case, we have

$$\begin{aligned}
e_{\Phi_i} &= \left\| \mathcal{B}_i(\mathbf{Q}_j^{(1)}) - \mathcal{B}_i(\mathbf{Q}_j^{(2)}) \right\|_F \\
&= \left\| \mathbf{V}_{ij} \mathcal{B}_{r_i}(\mathbf{Q}_j^{(1)}) \mathbf{V}_{ij}^\dagger - \mathbf{V}_{ij} \mathcal{B}_{r_i}(\mathbf{Q}_j^{(2)}) \mathbf{V}_{ij}^\dagger \right\|_F \\
&\leq \rho(\mathbf{V}_{ij}^\dagger \mathbf{V}_{ij}) \left\| \mathcal{B}_{r_i}(\mathbf{Q}_j^{(1)}) - \mathcal{B}_{r_i}(\mathbf{Q}_j^{(2)}) \right\|_F \tag{77}
\end{aligned}$$

$$\begin{aligned}
&= \left\| \mathcal{B}_{r_i}(\mathbf{Q}_j^{(1)}) - \mathcal{B}_{r_i}(\mathbf{Q}_j^{(2)}) \right\|_F \\
&\leq \frac{\beta}{\gamma_j} \left(1 + \beta \eta_{jj} P_j \rho(\mathbf{H}_{jj}^\dagger \mathbf{H}_{jj}) \right) \rho(\mathbf{H}_{jj}^\dagger \mathbf{H}_{jj}) \rho(\widetilde{\mathbf{H}}_{ij}^{-\dagger} \widetilde{\mathbf{H}}_{ij}^{-1}) \left\| \mathbf{Q}_j^{(1)} - \mathbf{Q}_j^{(2)} \right\|_F \tag{78} \\
&= \frac{\beta}{\gamma_j} \left(1 + \beta \eta_{jj} P_j \rho(\mathbf{H}_{jj}^\dagger \mathbf{H}_{jj}) \right) \rho(\mathbf{H}_{jj}^\dagger \mathbf{H}_{jj}) \rho(\widetilde{\mathbf{H}}_{ij}^{-\dagger} \widetilde{\mathbf{H}}_{ij}^{-1}) e_j
\end{aligned}$$

where (77) follows from the the triangle inequality $\|\mathbf{A}\mathbf{X}\mathbf{A}^\dagger\|_F \leq \rho(\mathbf{A}^\dagger \mathbf{A}) \|\mathbf{X}\|_F$; (78) follows from (74). The relationship between \mathbf{H}_{ij} and $\widetilde{\mathbf{H}}_{ij}$ implies that

$$\rho(\widetilde{\mathbf{H}}_{ij}^{-\dagger} \widetilde{\mathbf{H}}_{ij}^{-1}) = \rho(\mathbf{H}_{ij}^{-\dagger} \mathbf{H}_{ij}^{-1}). \tag{79}$$

The rest of the proof can then be completed following the same steps in Lemma 4.

REFERENCES

- [1] A. Sahai, G. Patel, c. dick, and A. Sabharwal, "On the impact of phase noise on active cancelation in wireless full-duplex," *IEEE Trans. Vel. Technol.*, vol. 62, no. 9, pp. 4494–4510, Nov. 2013.

- [2] E. Everett, D. Dash, C. Dick, and A. Sabharwal, "Self-interference cancellation in multi-hop full-duplex networks via structured signaling," in *Proc. 49th Annu. Allerton Conf. Commun., Control, Comput.*, Monticello, IL, Sep. 2011, pp. 1619–1626.
- [3] E. Everett, M. Duarte, C. Dick, and A. Sabharwal, "Empowering full-duplex wireless communication by exploiting directional diversity," in *Proc. 45th Asilomar Conf. Signals, Syst., Comput.*, Pacific Grove, CA, Nov. 2011, pp. 2002–2006.
- [4] D. Bharadia, E. McMillin, and S. Katti, "Full duplex radios," in *Proc. ACM SIGCOMM*. Hong Kong, China: ACM, 2013, pp. 375–386.
- [5] M. Vehkaperä, T. Riihonen, and R. Wichman, "Asymptotic analysis of full-duplex bidirectional mimo link with transmitter noise," in *IEEE Proc. 24th Int. Symp. Personal Indoor, Mobile Radio Commun. (PIMRC)*. IEEE, 2013, pp. 1265–1270.
- [6] B. Day, A. Margetts, D. Bliss, and P. Schniter, "Full-duplex bidirectional mimo: Achievable rates under limited dynamic range," *IEEE Trans. Signal Process.*, vol. 60, no. 7, pp. 3702–3713, Jul. 2012.
- [7] M. Duarte, C. Dick, and A. Sabharwal, "Experiment-driven characterization of full-duplex wireless systems," *IEEE Trans. Wireless Commun.*, vol. 11, no. 12, pp. 4296–4307, Dec. 2012.
- [8] A. C. Cirik, R. Wang, Y. Hua, and M. Latva-aho, "Weighted sum-rate maximization for full-duplex mimo interference channels," *Communications, IEEE Transactions on*, vol. 63, no. 3, pp. 801–815, 2015.
- [9] G. Scutari, D. P. Palomar, and S. Barbarossa, "Competitive design of multiuser mimo systems based on game theory: A unified view," *Selected Areas in Communications, IEEE Journal on*, vol. 26, no. 7, pp. 1089–1103, 2008.
- [10] —, "The mimo iterative waterfilling algorithm," *Signal Processing, IEEE Transactions on*, vol. 57, no. 5, pp. 1917–1935, 2009.
- [11] D. P. Palomar and Y. C. Eldar, *Convex optimization in signal processing and communications*. Cambridge university press, 2010.
- [12] X. Shang, B. Chen, and H. Poor, "Multiuser mimo interference channels with single-user detection: Optimality of beamforming and the achievable rate region," *IEEE Trans. Inf. Theory*, vol. 57, no. 7, pp. 4255–4273, Jul. 2011.
- [13] S. Boyd and L. Vandenberghe, *Convex optimization*. Cambridge, U.K.: Cambridge University Press, 2004.
- [14] E. Telatar, "Capacity of multi-antenna gaussian channels," *European Trans. on Telecommun.*, vol. 10, no. 6, pp. 585–595, 1999.
- [15] T. M. Cover and J. A. Thomas, *Elements of information theory*, 2nd ed. Hoboken, NJ: John Wiley & Sons, 2006.
- [16] R. Mochaourab and E. Jorswieck, "Optimal beamforming in interference networks with perfect local channel information," *IEEE Trans. Signal Process.*, vol. 59, no. 3, pp. 1128–1141, Mar. 2011.
- [17] E. A. Jorswieck, E. G. Larsson, and D. Danev, "Complete characterization of the pareto boundary for the

- miso interference channel,” *IEEE Trans. Signal Process.*, vol. 56, no. 10, pp. 5292–5296, 2008.
- [18] R. Zhang and S. Cui, “Cooperative interference management with miso beamforming,” *IEEE Trans. Signal Process.*, vol. 58, no. 10, pp. 5450–5458, 2010.
- [19] X. Shang and B. Chen, “Achievable rate region for downlink beamforming in the presence of interference,” in *Proc. 41st Asilomar Conf. Signals, Syst., Comput.*, Nov. 2007, pp. 1684–1688.
- [20] H. Cox, R. M. Zeskind, and M. M. Owen, “Robust adaptive beamforming,” *IEEE Trans. Acoust., Speech, Signal Process.*, vol. 35, no. 10, pp. 1365–1376, 1987.
- [21] M. Shakil and M. Ahsanullah, “Record values of the ratio of rayleigh random variables,” *Pak. J. Statist.*, vol. 27, no. 3, pp. 307–325, 2011.
- [22] K. W. Shum, K. K. Leung, and C. W. Sung, “Convergence of iterative waterfilling algorithm for gaussian interference channels.” *IEEE Journal on Selected Areas in Communications*, vol. 25, no. 6, pp. 1091–1100, 2007.
- [23] D. P. Bertsekas, “Distributed asynchronous computation of fixed points,” *Mathematical Programming*, vol. 27, no. 1, pp. 107–120, 1983.
- [24] Y. Huang and D. Palomar, “Rank-constrained separable semidefinite programming with applications to optimal beamforming,” *IEEE Trans. Signal Process.*, vol. 58, no. 2, pp. 664–678, Feb. 2010.
- [25] R. P. Agarwal, M. Meehan, and D. O’Regan, *Fixed point theory and applications*. Cambridge university press, 2001, vol. 141.
- [26] C. R. Rao and H. Yanai, “Generalized inverse of linear transformations: A geometric approach,” *Linear algebra and its applications*, vol. 66, pp. 87–98, 1985.
- [27] A. Hjørungnes and D. Gesbert, “Complex-valued matrix differentiation: Techniques and key results,” *Signal Processing, IEEE Transactions on*, vol. 55, no. 6, pp. 2740–2746, 2007.
- [28] R. A. Horn and C. R. Johnson, *Matrix analysis*. Cambridge university press, 2012.